ANESTHESIOLOGY

Positive Regulatory Domain I–binding Factor 1 Mediates Peripheral Nerve Injury–induced Nociception in Mice by Repressing Kv4.3 Channel Expression

Cunjin Wang, M.D., Ph.D., Yuchen Pan, M.D., Wenwen Zhang, Ph.D., Ying Chen, Ph.D., Chuhan Li, B.S., Fang Zhao, Ph.D., Thomas Behnisch, Ph.D.

Anesthesiology 2021; 134:435–56

EDITOR'S PERSPECTIVE

What We Already Know about This Topic

- The hyperexcitability of sensory neurons contributes to chronic pain after nerve injury
- The diminished expression of membrane-stabilizing potassium ion channels contributes to this hyperexcitability

What This Article Tells Us That Is New

- After nerve injury in mice, the enhanced expression of the positive regulatory domain I–binding factor 1 (PRDM1) reduced the expression of the Kv4.3 potassium ion channel
- The reduced expression of Kv4.3 caused nociceptive sensitization in male and female mice
- Conversely, maneuvers that enhanced Kv4.3 expression reduced nociceptive sensitivity in mice, suggesting that this regulatory pathway may have central importance in pain after nerve injury

ABSTRACT

Background: The transcriptional repressor positive regulatory domain I–binding factor 1 (PRDM1) is expressed in adult mouse dorsal root ganglion and regulates the formation and function of peripheral sensory neurons. The authors hypothesized that PRDM1 in the dorsal root ganglion may contribute to peripheral nerve injury–induced nociception regulation and that its mechanism may involve Kv4.3 channel transcriptional repression.

Methods: Nociception was induced in C57BL/6 mice by applying chronic constriction injury, complete Freund's adjuvant, or capsaicin plantar injection. Nociceptive response was evaluated by mechanical allodynia, thermal hyperalgesia, cold hyperalgesia, or gait analysis. The role of PRDM1 was evaluated by injection of *Prdm1* knockdown and overexpression adeno-associated viruses. The interaction of PRDM1 at the Kv4.3 (*Kcnd3*) promoter was evaluated by chromatin immunoprecipitation assay. Excitability of dorsal root ganglion neurons was evaluated by whole cell patch clamp recordings, and calcium signaling in spinal dorsal horn neurons was evaluated by *in vivo* two-photon imaging.

Results: Peripheral nerve injury increased PRDM1 expression in the dorsal root ganglion, which reduced the activity of the Kv4.3 promoter and repressed Kv4.3 channel expression (injured *vs.* uninjured; all $P < 0.001$). Knockdown of PRDM1 rescued Kv4.3 expression, reduced the high excitability of injured dorsal root ganglion neurons, and alleviated peripheral nerve injury–induced nociception (short hairpin RNA *vs.* Scram; all $P < 0.05$). In contrast, PRDM1 overexpression in naive mouse dorsal root ganglion neurons diminished Kv4.3 channel expression and induced hyperalgesia (PRDM1 overexpression *vs.* control, mean ± SD; n = 13; all $P < 0.0001$) as evaluated by mechanical allodynia (0.6 ± 0.3 *vs.* 1.2 ± 0.2 g), thermal hyperalgesia (5.2 ± 1.3 *vs.* 9.8 ± 1.7 s), and cold hyperalgesia (3.4 ± 0.5 *vs.* 5.3 ± 0.6 s). Finally, PRDM1 downregulation in naive mice reduced the calcium signaling response of spinal dorsal horn neurons to thermal stimulation.

Conclusions: PRDM1 contributes to peripheral nerve injury–induced nociception by repressing Kv4.3 channel expression in injured dorsal root ganglion neurons.

(ANESTHESIOLOGY 2021; 134:435–56)

Pain is a double-edged sword. Normal pain perception enables the body to respond to noxious stimuli, whereas abnormal pain perception is pathologic. For example, congenital pain insensitivity prevents perception of noxious stimuli, resulting in bruises, with potential life-threatening consequences; on the other hand, chronic pain causes long-term suffering and reduces quality of life. Neuropathic pain, which is caused by injury or disease of the somatosensory nervous system, is characterized by spontaneous pain, hyperalgesia, tactile allodynia, and paresthesia. Peripheral nerve injury can cause neuroma formation, and innocuous

This article is featured in "This Month in Anesthesiology," page 1A. Supplemental Digital Content is available for this article. Direct URL citations appear in the printed text and are available in both the HTML and PDF versions of this article. Links to the digital files are provided in the HTML text of this article on the Journal's Web site (www.anesthesiology.org). This article has a visual abstract available in the online version. C.W., Y.P., and W.Z. contributed equally to this article.

Submitted for publication May 18, 2020. Accepted for publication November 17, 2020. Published online first on December 28, 2020. From the Institutes of Brain Science, State Key Laboratory of Medical Neurobiology and Ministry of Education Frontiers Center for Brain Science, Fudan University, Shanghai, China (C.W., W.Z., Y.C., C.L., F.Z., T.B.); The Yangzhou Clinical College of Xuzhou Medical University and Department of Anesthesiology, Northern Jiangsu People's Hospital, Yangzhou, China (C.W.); Department of Neurology, Jiangsu Provincial Corps Hospital, Chinese People's Armed Police Force, Yangzhou, China (Y.P.); and Institute of Neuroscience, Key Laboratory of Molecular Neurobiology of the Ministry of Education and the Collaborative Innovation Center for Brain Science, Second Military Medical University, Shanghai, China (Y.P.).

 Anesthesiology 2021; 134:435–56. DOI: 10.1097/ALN.0000000000003654

<zdoi;. DOI: 10.1097/ALN.0000000000003654>

external stimulation of the skin at the area of nerve injury may induce hyperexcitability or ectopic spontaneous discharge of primary sensory neurons in the injured dorsal root ganglion.[1]

Reduction in A-type voltage-gated K^+ currents is one of the major causes of abnormal excitability of injured sensory neurons of the dorsal root ganglion.[2,3] The voltage-gated K^+ channel primarily mediates outward currents, resulting in repolarization of the cell membrane. Peripheral nerve injury leads to sustained decreases in voltage-gated K^+ channel expression, which may cause abnormal dorsal root ganglion neuron excitability and neuropathic pain.[4] However, little is known about the transcriptional regulatory mechanism of persistent voltage-gated K^+ channel decrease in the injured dorsal root ganglion.

Positive regulatory domain I–binding factor 1 (PRDM1) belongs to the PRDI-BF1 and RIZ homology domain–containing family of transcriptional repressors, which are characterized by the presence of Krüppel-type zinc fingers and a positive regulatory domain at the N terminus. PRDM1 can directly bind to DNA promoter regions or act as a scaffold protein to recruit corepressor proteins, including histone-modifying enzymes (histone methyltransferase and histone deacetylases).[5,6] PRDM1 plays roles in the adaptive immune response, tumorigenesis, and embryonic development.[7–9] In the nervous system, PRDM1 promotes the development of sensory neurons,[10] and it is expressed in peripheral sensory neurons of the dorsal root ganglion in adult mice.[11] In the current study, we sought to determine whether PRDM1 may have a role in pain hypersensitivity and to characterize its mechanism of action. The primary outcome was the effect of knockdown of dorsal root ganglion PRDM1 on nociceptive behavior after peripheral nerve injury.

Materials and Methods

Animals

C57BL/6 male and female mice weighing 25 to 30 g were obtained from Jie Si Jie Experimental Animal Co., Ltd. (China) and maintained in accordance with the established standards of animal care and procedures of the Institutes of Brain Science and State Key Laboratory of Medical Neurobiology (approval No. 31320103906; Fudan University, Shanghai, China). In addition, all experimental protocols were approved by the Medical Experimental Animal Administrative Committee of Fudan University (Shanghai, China) and were conducted in accordance with the ethical guidelines of the National Institutes of Health (Bethesda, Maryland) and the International Association for the Study of Pain (Washington, D.C.) for care and use of laboratory animals under pain research.[12] Animals were numbered, randomly assigned to different experimental groups using a random number table, and tested in sequential order. All efforts were made to minimize the number of animals used as well as their suffering. After experimentation, the mice were euthanized *via* carbon dioxide inhalation. All behavioral tests, electrophysiologic recordings, calcium imaging, and biochemical experiments were performed by experimenters who were blinded to the treatments. All experiments were conducted between 9:00 AM and 6:00 PM.

Animal Models

The chronic constriction injury–induced nociception model, a common model for nerve injury, was carried out according to previously published methods.[13] Briefly, the mice were anesthetized with 40 mg/kg sodium pentobarbital. The left common sciatic nerve was exposed and then loosely ligated with 6-0 silk threads at the sciatic nerve bifurcation at intervals of approximately 1 mm. The sham group also underwent sciatic nerve exposure but without ligation. The complete Freund's adjuvant–induced nociception model, a model for inflammation-associated acute pain induction, was established in mice as described previously.[14] In brief, 15 μl of complete Freund's adjuvant (1 mg/ml; Sigma-Aldrich, USA) was subcutaneously injected into the left hind paw, and 15 μl of saline was injected as a control. The capsaicin-induced acute pain mouse model was established as described previously.[15] In brief, 10 μl of vehicle (10% ethanol and 10% Tween 80 in saline) containing 1 μg capsaicin (Sigma-Aldrich) or 10 μl of vehicle alone was injected into the plantar surface of the left hind paw.

Mechanical Allodynia

Mechanical allodynia was assessed using Von Frey hair (Stoelting, USA) testing to measure the paw withdrawal threshold. The mice were placed in a Plexiglas cage with a wire mesh floor and were allowed to habituate for 30 min before testing. This habituation was continued for 2 to 3 days, and during this time, the basal pain hypersensitivity threshold was recorded. Measurements were performed according to the previously published method.[16] Briefly, a series of calibrated Von Frey hairs (0.04, 0.07, 0.16, 0.4, 0.6, 1.0, and 1.4 g) were used to vertically stimulate the central part of the plantar surface of the hind paw. The response to each hair was measured five times at 5-min intervals. The paw withdrawal threshold was defined as the lowest hair force in grams that produced at least three withdrawal responses in five tests.

Thermal Hyperalgesia

Thermal hyperalgesia was measured using an IITC Plantar Analgesia (IITC Life Science Inc., USA) to measure the paw withdrawal latency.[17] The mice were placed into Plexiglas chambers with a temperature-controlled glass platform. The heat source was focused on the central part of the plantar surface of the hind paw. The stimulus was shut off when the hind paw moved or after 20 s to prevent tissue damage. The time from the onset of radiant heat to the endpoint

was the paw withdrawal latency. The radiant heat intensity was adjusted to obtain a basal paw withdrawal latency of 10 to 12 s. Thermal stimuli were delivered three times to each hind paw at 5-min intervals.

Cold Hyperalgesia

Measurements of cold hyperalgesia were based on a previously published method.[18] Powdered dry ice was compacted into the barrel of a 12-mm-diameter plastic syringe and used to deliver a cold stimulus to the plantar surface. Briefly, mice were enclosed in individual Plexiglas chambers on an elevated glass platform that was 2.5 mm thick, and cold stimulation was delivered to the animal's plantar hind paw from below. Care was taken to ensure a smooth surface of the dry ice, and light pressure was applied to make contact between the dry ice and the glass. The withdrawal latency was measured with a stopwatch. Withdrawal was defined as any action to move the paw away from the cold glass. The maximum time allowed for withdrawal was 20 s to avoid potential tissue damage, and cold stimuli were delivered three times to each hind paw at 5-min intervals.

Rotarod Test

Mice were placed on a moving rotarod (Ugo Basile, Italy) programmed to accelerate from 5 to 40 revolutions per minute, over 300 s. After 3 days of training, the time the mice managed to remain on the rotarod was averaged over three consecutive trials.

CatWalk Automated Gait Analysis

The CatWalk XT system (Noldus Information Technology, The Netherlands) was used for quantitative assessment of gait parameters and footfalls in rodents. CatWalk is a verified system in the research of several pain models, such as spinal cord injury, osteoarthritis, and neuropathic pain, and has proven to be a reliable method for measuring nonreflexive nociceptive-associated behavior.[19,20] The test involves mice passing through a dark tunnel with a glass plate from one side to the other. Their footprints are illuminated by fluorescent light from the glass plate and captured by a high-speed camera positioned underneath the plate. The captured images are processed by CatWalk XT software. Data were considered for mice that passed through the camera's photographing area between 0.5 and 5 s and within a maximum run variation of 60% or less. The print area (the contacting area between the hind paw and glass) and the single stance (the duration of the contralateral or ipsilateral hind paw touching the glass plate in the step cycle) were measured to assess nociceptive response.

Dorsal Root Ganglion and Intraspinal Microinjection

Dorsal root ganglion microinjection was performed as described previously.[21] Briefly, the mice were anesthetized with sodium pentobarbital, a midline incision was made in the lower lumbar back region, and the lumbar articular process was exposed and removed. The exposed dorsal root ganglion was injected with adeno-associated virus 5 containing PRDM1 short hairpin RNA and a green fluorescent protein expression marker (adeno-associated virus 5–PRDM1–short hairpin RNA–green fluorescent protein; 3.4E + 12 virus genomes [v.g.]/ml); adeno-associated virus 5–scrambled–short hairpin RNA–green fluorescent protein (3.7E + 12 v.g./ml); adeno-associated virus 5–human synapsin–PRDM1-3×Flag (3.8E + 12 v.g./ml); or adeno-associated virus 5–human synapsin–green fluorescent protein (3.4E + 12 v.g./ml) viral solution (0.5 μl) through a glass micropipette connected to a micro syringe with heat glue and filled with mineral oil. The pipette remained 10 min after injection. The short hairpin RNA targeting the sequence of mouse PRDM1 (Gene Bank Accession NM_007548.4) was designed as follows: 5'-GCATTAGTTCCAATGGCTT-3'. A scrambled sequence was also designed as a negative control (Scram): 5'-CGCTGAGTACTTCGAAATGTC-3'. The adeno-associated virus vectors were designed and generated by Shanghai Taitool Bioscience (China). Intraspinal injection was performed as described previously.[22] The mice underwent hemilaminectomy at the thoracic 13–lumbar 1 vertebral segments. After exposure of the spinal cord, each mouse received adeno-associated virus 5–human synapsin–GCaMP6s (6.5E + 12 v.g./ml) viral solution (0.5 μl). The tip of the glass micropipette reached the superficial laminae of the spinal dorsal horn.

Reverse Transcription Quantitative Polymerase Chain Reaction

Dorsal root ganglions were lysed with TRIzol reagent (Invitrogen, United Kingdom), and total RNA was extracted according to the manufacturer's instructions. The mRNA level was then measured using reverse transcription quantitative polymerase chain reaction performed with SYBR Green real-time polymerase chain reaction Mater Mix (Toyobo, Japan). Gene expression was normalized to the expression of the standard housekeeping gene glyceraldehyde-3-phosphate dehydrogenase using the ΔΔCT method. Polymerase chain reaction was performed under the following conditions: 95°C for 3 min followed by 45 cycles at 95°C for 10 s, 65°C for 30 s, 72°C for 10 s, and 72°C for 10 min. Primer sequences are listed in Supplemental Digital Content 1 (http://links.lww.com/ALN/C522).

Immunohistochemistry

Mice were deeply anesthetized with sodium pentobarbital and perfused with 4% paraformaldehyde. The lumbar 4 and lumbar 5 dorsal root ganglions were harvested. Dorsal root ganglion sections were cut on a cryostat (Leica 1900, Leica, Germany) and mounted onto slides for immunofluorescence. After being blocked with 5% donkey serum

and 0.5% Triton X-100 for 2 h at room temperature, the sections were incubated overnight at 4°C with primary antibodies, including rabbit anti-PRDM1 (1:200, Cell Signaling, USA), mouse anti-NeuN (1:200, EMD Millipore, Germany), mouse anti–glutamine synthetase (1:200, EMD Millipore), mouse anti–calcitonin gene-related peptide (1:200, Abcam, USA), biotinylated isolectin B4 (1:400, Sigma-Aldrich), mouse anti–neurofilament-200 (1:400, Sigma-Aldrich), mouse anti-Kv4.3 (1:100, Sigma-Aldrich), and chicken anti–green fluorescent protein (1:3,000, Aves Labs). Sections were then incubated in Alexa Fluor 488– or Alexa Fluor 594–conjugated secondary antibodies (1:200, Thermal Scientific, USA) containing Hoechst for 2 h at room temperature. Images of samples were collected using confocal microscopy (FluoView FV1000; Olympus, Japan). The numbers of PRDM1-positive neurons were calculated manually or using National Institutes of Health ImageJ Software.

Western Blot Analysis

After mice were deeply anesthetized with sodium pentobarbital, the unilateral lumbar 4 and lumbar 5 dorsal root ganglions were removed and immediately frozen in liquid nitrogen. The dorsal root ganglions were ground in cold (4°C) radioimmunoprecipitation assay lysis buffer (Beyotime Institute of Biotechnology, China) containing a cocktail of protease inhibitors. After incubation on ice for 15 min, homogenates were centrifuged at 12,000*g* for 20 min at 4°C. Protein concentrations were measured using a BCA Protein Assay Kit (Beyotime Institute of Biotechnology). Protein samples were then denatured at 95°C and separated by 10% sodium dodecyl sulphate-polyacrylamice gel electrophoresis. After the samples were transferred to polyvinylidene fluoride membranes and blocked with 5% nonfat milk, the membranes were incubated overnight at 4°C with primary antibodies, including rabbit anti-PRDM1 (1:200, Cell Signaling), rabbit anti-Kv4.3 (1:1,000, Alomone Lab, Israel), mouse anti-Flag (1:1,000, GNI, Japan), and rabbit anti–glyceraldehyde-3-phosphate dehydrogenase (1:1,000, Cell Signaling). The membranes were then incubated with horseradish peroxidase–conjugated anti-mouse or anti-rabbit secondary antibodies for 2 h at room temperature. Signals were finally detected using enhanced chemiluminescence (Pierce), and the bands were visualized with the FluorChem E system (ProteinSimple, USA).

RNA Sequencing Analysis

Total RNA was extracted using the miRNeasy Mini Kit (Qiagen, GmBH, Germany) according to the manufacturer's instructions, and the RNA integrity number was assessed by an Agilent Bioanalyzer 2100 (Agilent Technologies, USA). Qualified total RNA was further purified using the RNAClean XP Kit (Beckman Coulter, Inc., USA) and RNase-Free DNase Set (Qiagen, GmBH). RNA sequencing libraries were prepared according to the Illumina TruSeq protocol (Illumina, USA). Levels of gene expression were determined using edgeR software (Illumina),[23] with discovery rate adjustment, and were reported in fragments per kilobase of transcript per million mapped reads. A gene was considered to be expressed if it had a fragments per kilobase per million greater than 1. For a gene to be called differentially expressed, it had to meet two criteria: a greater than 2.0-fold expression level change and P value < 0.05.

Chromatin Immunoprecipitation Assay

Fresh dorsal root ganglions were rapidly removed from anesthetized mice and stabilized for 3 min using stabilization buffer. Then, the dorsal root ganglions were incubated in 1% formaldehyde for 20 min at room temperature, and the reaction was stopped by adding glycine. After being washed three times with phosphate-buffered saline, the dorsal root ganglions were incubated in lysis buffer for 30 min on ice. Finally, the dorsal root ganglions were sonicated (30 s on: 30 s off) in chromatin immunoprecipitation dilution buffer using a water bath sonicator at 4°C for 10 min. Chromatin was pulled down using the following antibodies: nonspecific mouse immunoglobulin G (Bangs Laboratories, USA) and PRDM1 (Cell Signaling). Ten percent of the sample for immunoprecipitation was used as input. After chromatin precipitation, quantitative polymerase chain reaction was performed using the primers shown in Supplemental Digital Content 2 (http://links.lww.com/ALN/C523).

Tissue Clearing and Three-dimensional Imaging

Clearing of the dorsal root ganglion and spinal cord with clear, unobstructed brain imaging cocktails was performed as described previously.[24] After fixation with 4% paraformaldehyde overnight, dorsal root ganglion and spinal cord samples were washed three times with phosphate-buffered saline for 1 h each with shaking at room temperature. The samples were then cleared with 1/2-Reagent-1 (a 1:1 mixture of Reagent-1 [urea, quadrol, Triton X-100, and distilled H_2O] and phosphate-buffered saline), with shaking at 60 revolutions per minute at 37°C for 3 h. Reagent-1 was applied for further clearing under the same conditions and replaced every 2 days until distinct optical transparency was achieved. The samples were then washed with phosphate-buffered saline with gentle shaking three times at room temperature for 1 h each. The samples were incubated with 4',6-diamidino-2-phenylindole with shaking at 60 revolutions per minute at 37°C for 24 h followed by three washes with phosphate-buffered saline with shaking at room temperature for 1 h each. The 1/2-Reagent-2 (a 1:1 mixture of Reagent-1 [urea, sucrose, triethanolamine, and distilled H_2O] and phosphate-buffered saline) was then applied to clear the sample a final time with shaking at 60 revolutions per minute at 37°C for 24 h, and Reagent-2

was applied for further clearing and replaced every day until distinct optical transparency was achieved. All clearing procedures were performed in darkness to avoid fluorescence bleaching.

Image Acquisition. Three-dimensional images of transparent dorsal root ganglion and spinal cord samples were acquired using a light-sheet microscope (Lightsheet Z.1, Carl Zeiss, Germany). All images were processed with Imaris 9 (Bitplane, Switzerland) or Arivis (Vision4D, Germany), and surface visualization was used for three-dimensional rendering.

Whole Cell Patch Clamp Recordings

Four weeks after viral injection into the dorsal root ganglions, freshly dissociated dorsal root ganglion cultures were prepared. Cells were placed on glass coverslips coated with poly-D-lysine and grown in neurobasal-defined medium at 37°C with 5% CO_2 for 24 h before experiments. Whole cell current clamp recordings were performed at room temperature to measure action potentials and the resting membrane potential with an Axonpatch 200B amplifier and a Digidata 1440A digitizer (Axon Instruments, USA). The recording chamber (300 μl) was continuously superfused at a flow rate of 1 to 2 ml/min. Series resistance was compensated (>80%), and leak subtraction was performed. Only green fluorescent protein–positive cells were selected for study. The pipette solution contained the following (in mM): 126 K-gluconate, 10 NaCl, 1 $MgCl_2$, 10 EGTA, 2 Na-ATP, and 0.1 Mg-GTP, adjusted to pH 7.3 with KOH. The external solution contained the following (in mM): 140 NaCl, 5 KCl, 2 $CaCl_2$, 1 $MgCl_2$, 10 N-2-hydroxyethylpiperazine-N-2-ethane sulfonic acid, and 10 glucose, adjusted to pH 7.4 with NaOH. In current clamp experiments, the action potentials were evoked by current injection steps. The resting membrane potential was measured without a current injection.

In Vivo Ca^{2+} Imaging

For *in vivo* Ca^{2+} imaging, GCaMP6s-expressing mice were anesthetized by sodium pentobarbital supplemented with 1 to 2% isoflurane in air if needed. Body temperatures were maintained at 37°C with a heating blanket. The skin was incised at the thoracic 12–lumbar 2 level. The paravertebral muscle overlying thoracic 12–lumbar 2 was removed. The laminectomy was performed at thoracic 13–lumbar 1, and a custom-made spinal chamber was attached. The laminectomized region was then covered with agarose (type III-A, Sigma-Aldrich; 1% in Ringer solution), and a glass coverslip was placed to seal the laminectomized area. Two-photon Ca^{2+} imaging was performed using an Olympus FVMPE-RS with a 25 × 1.05 WMP water-immersion lens, and the fluorescence signals were measured at a frame scanning rate of 30 Hz (512 × 512 pixel images). The InSight X3 laser (Spectra Physics, USA) was tuned at 920 nm for two-photon excitation of GCaMP6s. Movies were imported into ImageJ (http://rsbweb.nih.gov/ij/), and fluorescence traces were analyzed from somatic regions of interest and expressed as relative percentage changes (Δfluorescence/fluorescence) after background subtraction. Thermal pain stimulation was performed using a custom-built heating plate applied to the plantar surface of the hind paw. The temperature of the heating plate was increased from a baseline temperature of 25°C to 45°C or decreased from 45°C to 25°C. Temperature changes occurred as a ramp of 0.7°C/s to the target temperature of 45°C (maintained for 10 s) before returning to baseline.

Statistical Analysis

Data are presented as mean ± SD. No formal *a priori* statistical power calculations were conducted, and the sample sizes were based on our previous knowledge and experience with this design. There were no missing data. All data from different groups were verified for normality and homogeneity of variance using Kolmogorov–Smirnov and Brown–Forsythe tests before analysis. For pain hypersensitivity behavioral experiments, differences between groups for threshold, latency, print area, and single stance results were determined using two-way repeated-measures ANOVA followed by the *post hoc* Bonferroni multiple comparison test. For reverse transcription quantitative polymerase chain reaction, Western blot, and chromatin immunoprecipitation–quantitative polymerase chain reaction experiments, group differences were determined using paired or independent unpaired two-tailed Student's *t* tests and one-way ANOVA followed by the Tukey *post hoc* test. Electrophysiologic data were tested using two-way ANOVA (for multiple time points) followed by *post hoc* Bonferroni or unpaired two-tailed Student's *t* tests. For *in vivo* Ca^{2+} imaging experiments, group differences were determined using unpaired two-tailed Student's *t* tests. Differences were considered statistically significant if $P < 0.05$. No outliers were observed, and no data were excluded from statistical analyses. All statistical analyses were performed using GraphPad Prism 7.0 software (GraphPad, USA).

Results

PRDM1 Expression Is Increased in the Dorsal Root Ganglion after Peripheral Nerve Injury

Peripheral nerve injury causes many molecular changes in the dorsal root ganglion, and these changes are critical for the development of neuropathic pain. To determine whether PRDM1 is modulated in response to peripheral nerve injury, we examined the expression of PRDM1 in the mouse dorsal root ganglion after chronic constriction injury.[13] Compared with the contralateral side, the ipsilateral (injured) lumbar 4 and lumbar 5 dorsal root ganglions expressed statistically higher levels of *Prdm1* mRNA on days

3 (fold change: 2.0 ± 0.8; two-tailed paired *t* test, $t_{(5)} = 4.01$; n = 6; $P = 0.032$) and 7 (fold change: 1.6 ± 0.6; two-tailed paired *t* test, $t_{(5)} = 4.30$; n = 6; $P = 0.022$) after chronic constriction injury (fig. 1A). As a control, sham surgery did not affect the basal mRNA expression level of *Prdm1* in ipsilateral lumbar 4 and lumbar 5 dorsal root ganglions (fig. 1B). Furthermore, PRDM1 protein was expressed at higher levels on days 3 (fold change: 3.1 ± 0.6; two-tailed paired *t* test, $t_{(5)} = 15.28$; n = 6; $P < 0.0001$) and 7 (fold change: 2.7 ± 0.6; two-tailed paired *t* test, $t_{(5)} = 12.28$; n = 6; $P < 0.0001$) but not on day 14 after chronic constriction injury (fig. 1C). As a control, sham surgery did not alter the basal expression of the protein level of PRDM1 in ipsilateral lumbar 4 and lumbar 5 dorsal root ganglion (fig. 1D). The number of PRDM1-positive neurons was also greater in the injured dorsal root ganglion compared with the dorsal root ganglion of the sham group on day 7 after chronic constriction injury (chronic constriction injury day 7: 81.5 ± 7.0% *vs.* sham day 7: 17.8 ± 3.1%; two-tailed unpaired *t* test, $t_{(10)} = 20.42$; n = 6; $P < 0.0001$; fig. 1, E and F).

We further examined whether other pain hypersensitivity models altered PRDM1 expression in the dorsal root ganglion. A similar increase in PRDM1 expression was found after plantar injection of complete Freund's adjuvant. The levels of *Prdm1* mRNA (Supplemental Digital Content 3, http://links.lww.com/ALN/C524, fig. S1A) and protein (Supplemental Digital Content 3, http://links.lww.com/ALN/C524, fig. S1, B and C) on days 3 and 7 after complete Freund's adjuvant injection on the injured side were higher than those on the contralateral side. However, saline injection did not change the basal expression of *Prdm1* mRNA (Supplemental Digital Content 3, http://links.lww.com/ALN/C524, fig. S1D) or protein (Supplemental Digital Content 3, http://links.lww.com/ALN/C524, fig. S1, E and F) in ipsilateral lumbar 4 and lumbar 5 dorsal root ganglions. We further determined whether acute pain also changes PRDM1 expression in the dorsal root ganglion by injecting capsaicin into the plantar side of the hind paw. Unexpectedly, the amount of PRDM1 protein was not altered in the ipsilateral lumbar 4 or lumbar 5 dorsal root ganglion (Supplemental Digital Content 3, http://links.lww.com/ALN/C524, fig. S1, G and H), suggesting that the response is limited to chronic pain.

To further characterize PRDM1 expression after nociceptive pain, we analyzed its distribution pattern in the mouse dorsal root ganglion. By co-labeling PRDM1 with NeuN (a neuronal marker) or glutamine synthetase (a marker for satellite glial cells) and Hoechst (a marker for cellular nuclei), we determined that PRDM1 was localized in the nuclei of dorsal root ganglion neurons (fig. 2A) and could not be detected in satellite glial cells (fig. 2B). We further examined the distribution of PRDM1 in various subpopulations of dorsal root ganglion neurons. The increased PRDM1 was mainly distributed among nociceptive neurons expressing three different marker proteins: calcitonin gene-related peptide (fig. 2C), isolectin B4 (fig. 2D), and neurofilament-200 (fig. 2E). We also performed a control experiment to verify PRDM1 antibody specificity *via* injection of short hairpin RNA in the mouse dorsal root ganglion (Supplemental Digital Content 4, http://links.lww.com/ALN/C525, fig. S2). Taken together, our results show that PRDM1 expression in dorsal root ganglion nociceptive neurons increases in the early stage of peripheral nerve injury.

PRDM1 Knockdown in the Dorsal Root Ganglion Increases the Pain Hypersensitivity Threshold in Naive Mice and Improves Peripheral Nerve Injury–induced Hyperalgesia

To determine the role of PRDM1 in normal pain perception and peripheral nerve injury–induced nociception in the dorsal root ganglion, we injected adeno-associated virus 5–expressing *Prdm1* short hairpin RNA or control scrambled short hairpin RNA (Scram) into ipsilateral lumbar 4 and lumbar 5 mouse dorsal root ganglions 4 weeks before chronic constriction injury and assessed nociceptive response (fig. 3A). Four weeks after the injection, we observed the expression of the virus in the dorsal root ganglion by immunofluorescence staining (Supplemental Digital Content 5, http://links.lww.com/ALN/C526, fig. S3A). We used tissue clearing technology to make the dorsal root ganglion transparent and performed three-dimensional image reconstruction to observe the expression of the virus in the dorsal root ganglion (Supplemental Digital Content 6, http://links.lww.com/ALN/C527). As expected, *Prdm1* short hairpin RNA reduced basal expression and blocked the chronic constriction injury–induced increase in PRDM1 protein expression in ipsilateral lumbar 4 and lumbar 5 dorsal root ganglion on day 7 after chronic constriction injury (fold change: naive + short hairpin RNA: 0.3 ± 0.2 *vs.* naive + Scram: 1.0 ± 0.4; chronic constriction injury + short hairpin RNA: 0.9 ± 0.2 *vs.* chronic constriction injury + Scram: 2.2 ± 0.7; one-way ANOVA; n = 6; $P < 0.001$; fig. 3, B and C) and mRNA (fold change: naive + short hairpin RNA: 0.3 ± 0.1 *vs.* naive + Scram: 1.0 ± 0.5; chronic constriction injury + short hairpin RNA: 1.2 ± 0.7 *vs.* chronic constriction injury + Scram: 1.9 ± 0.4; one-way ANOVA; n = 6; $P = 0.040$; fig. 3D). In behavioral assays, PRDM1 knockdown increased the paw withdrawal threshold to mechanical stimulation (short hairpin RNA: 3.5 ± 1.4 g *vs.* Scram: 1.2 ± 0.2 g; two-way ANOVA; n = 8; $P < 0.0001$; fig. 3E) and paw withdrawal latency to thermal (short hairpin RNA: 13.0 ± 0.9 s *vs.* Scram: 10.6 ± 1.6 s; two-way ANOVA; n = 8; $P = 0.021$; fig. 3F) or cold (short hairpin RNA: 6.9 ± 0.9 s *vs.* Scram: 5.2 ± 0.8 s; two-way ANOVA; n = 8; $P = 0.001$; fig. 3G) stimulation on the ipsilateral side in naive mice. PRDM1 knockdown also attenuated the hyperalgesia induced by chronic constriction injury. Consistently, injection of *Prdm1* short hairpin RNA also reduced the mechanical, thermal, and cold hyperalgesia caused by complete Freund's adjuvant injection

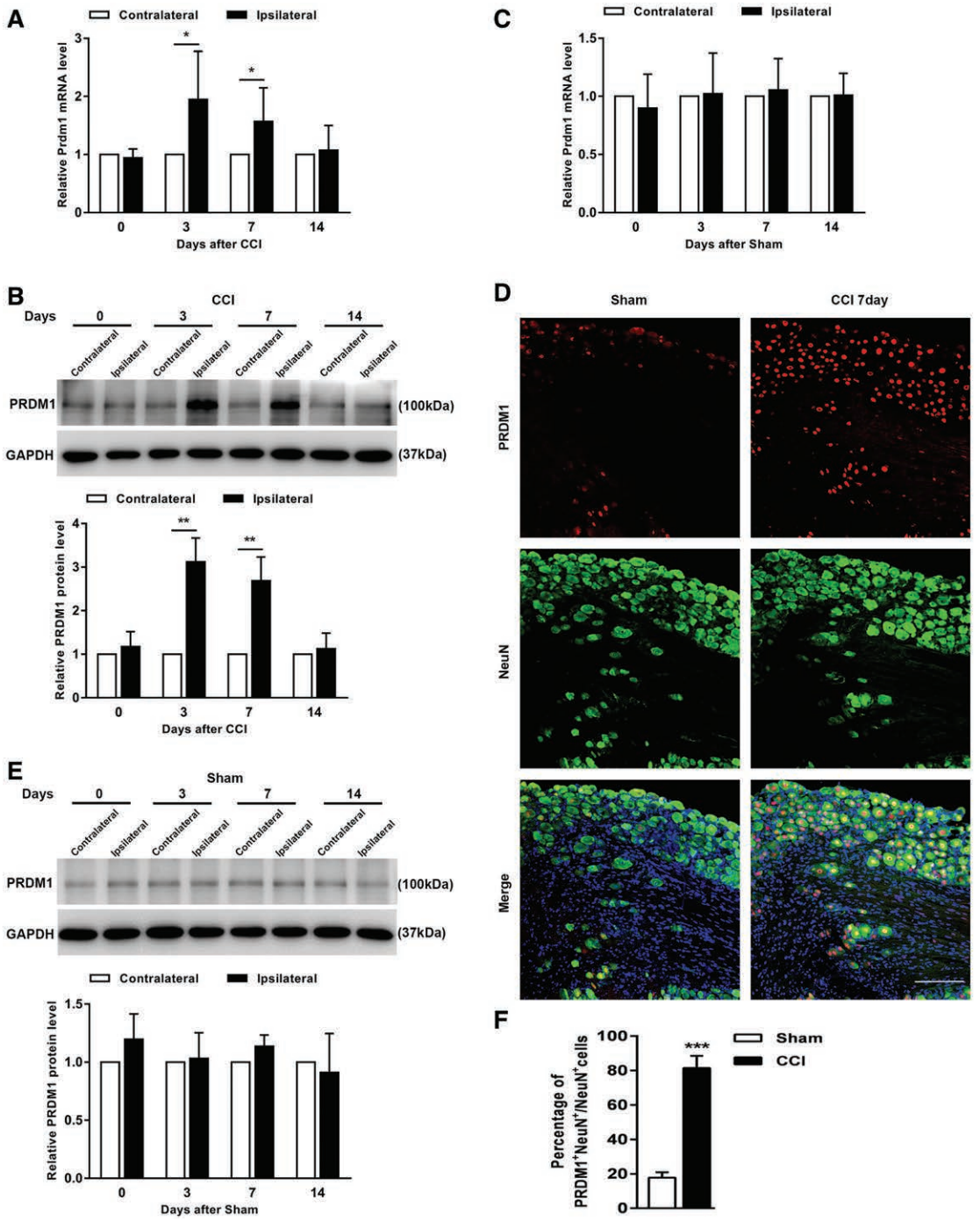

Fig. 1. Expression and cellular distributions of PRDM1 in the mouse dorsal root ganglion after chronic constriction injury surgery. (*A*) Reverse transcription quantitative polymerase chain reaction showing a time course of *Prdm1* mRNA expression in ipsilateral and contralateral lumbar 4 and lumbar 5 dorsal root ganglions after chronic constriction injury surgery. Data are expressed as mean ± SD. $^{*}P < 0.05$ *versus* the contralateral dorsal root ganglion by two-tailed paired *t* test, n = 6 per group. (*B*) Reverse transcription quantitative polymerase chain showing a time course of *Prdm1* mRNA in ipsilateral and contralateral lumbar 4 and lumbar 5 dorsal root ganglions after sham surgery. (*C*) Western blot analysis showing a time course for the expression of PRDM1 protein in ipsilateral and contralateral lumbar 4 and lumbar 5 dorsal root ganglions after chronic constriction injury surgery. Data are expressed as mean ± SD. $^{**}P < 0.01$ *versus* the contralateral dorsal root ganglion by two-tailed paired *t* test, n = 6 per group. (*D*) Western blot analysis showing a time course for the expression of PRDM1 protein in ipsilateral and contralateral lumbar 4 and lumbar 5 dorsal root ganglions after sham surgery. (*E* and *F*) Neurons labeled by PRDM1 and NeuN in ipsilateral lumbar 4 and lumbar 5 dorsal root ganglions on days 7 after chronic constriction injury or sham surgery. Data are expressed as mean ± SD. $^{***}P < 0.001$ *versus* the sham group by unpaired *t* test, n = 6 mice per group. *Scale bar*, 150 μm. PRDM1, positive regulatory domain I–binding factor 1.

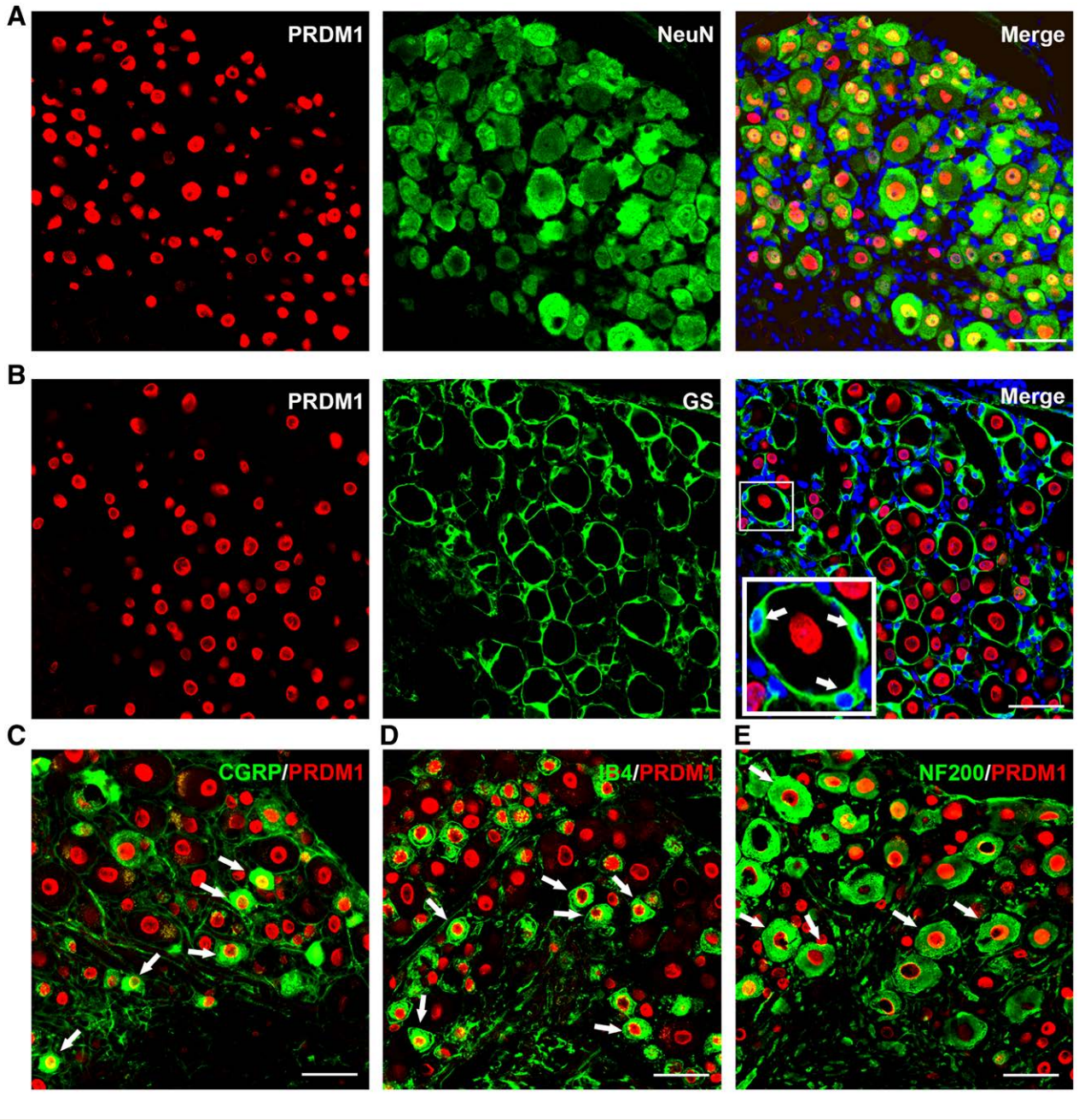

Fig. 2. Distribution of PRDM1 protein in the lumbar dorsal root ganglion of chronic constriction injury mice. (*A* and *B*) PRDM1 is coexpressed exclusively with NeuN in cellular nuclei (*A*) and is undetected in cellular nuclei of glutamine synthetase–labeled cells (*B*). (*C* through *E*) Expression of PRDM1 in calcitonin gene–related peptide– (*C*), isolectin B4– (*D*) and neurofilament-200– (*E*) positive neurons. *Scale bars*, 50 μm. PRDM1, positive regulatory domain I–binding factor 1.

(Supplemental Digital Content 5, http://links.lww.com/ALN/C526, fig. S3, B through D). However, dorsal root ganglion injection or knockdown of PRMD1 did not alter mouse motor activity (Supplemental Digital Content 5, http://links.lww.com/ALN/C526, fig. S3E).

In addition, we employed CatWalk gait analysis to evaluate nonreflexive nociceptive behavior after knockdown of PRMD1 in dorsal root ganglion. We measured alterations in two parameters for the ipsilateral hind paw of chronic constriction injury mice: the print area and the single stance (% ipsilateral/contralateral). Our results showed that PRDM1 knockdown reversed the chronic constriction injury–induced decrease in the print area (short hairpin RNA: 83.1 ± 14.3% *vs.* Scram: 21.8 ± 19.0%; two-way ANOVA; n = 8;

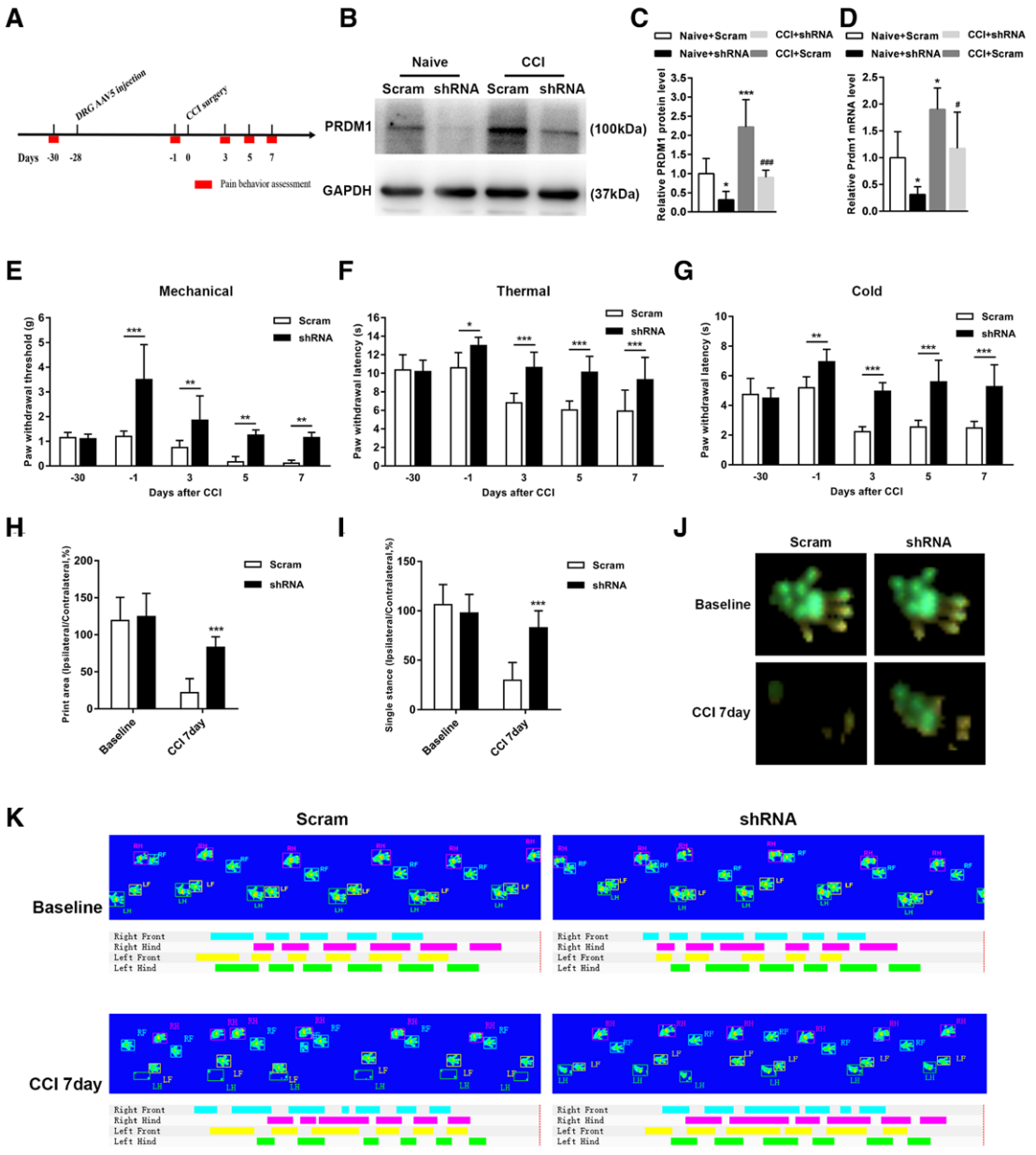

Fig. 3. Dorsal root ganglion PRDM1 knockdown increases the nociceptive response threshold in naive mice and attenuates chronic constriction injury–induced nociception development in mice. (*A*) A schematic map of the pain behavior assessment. (*B* and *C*) Levels of PRDM1 protein in ipsilateral lumbar 4 and lumbar 5 dorsal root ganglions on day 7 after chronic constriction injury in chronic constriction injury or naive mice injected with adeno-associated virus 5–Prdm1 short hairpin RNA or adeno-associated virus 5–control scrambled short hairpin RNA (Scram). Data are expressed as mean ± SD. $^{*}P < 0.05$ and $^{***}P < 0.001$ *versus* the corresponding naive + Scram group, $^{\#\#\#}P < 0.001$ *versus* the corresponding chronic constriction injury + Scram group. One-way ANOVA followed by *post hoc* Tukey test, $F_{(3, 20)} = 20.62$, n = 6 per group. (*D*) Level of *Prdm1* mRNA in ipsilateral lumbar 4 and lumbar 5 dorsal root ganglions on day 7 after chronic constriction injury in chronic constriction injury or naive mice injected with short hairpin RNA or Scram. Data are expressed as mean ± SD. $^{*}P < 0.05$ *versus* the corresponding naive + Scram group. $^{\#}P < 0.05$ *versus* the corresponding chronic constriction injury + Scram group. One-way ANOVA followed by *post hoc* Tukey test, $F_{(3, 20)} = 11.75$, n = 6 per group. (*E* through *G*) The effect of microinjection of short hairpin RNA or Scram into ipsilateral lumbar 4 and lumbar 5 dorsal root ganglions on paw withdrawal responses to mechanical (*E*), thermal (*F*), and cold (*G*) stimuli on the ipsilateral side at the indicated days before or after chronic constriction injury surgery in mice. Data are expressed as mean ± SD. $^{*}P < 0.05$, $^{**}P < 0.01$, and $^{***}P < 0.001$ *versus* the Scram group by two-way ANOVA followed by *post hoc* Bonferroni multiple comparison test, $F_{(4, 70)} = 8.32$ (*E*), $F_{(4, 70)} = 4.52$ (*F*), and $F_{(4, 70)} = 9.11$ (*G*), n = 8 per group. (*H* and *I*) Percentage of the ipsilateral paw print area (*H*) and single stance (*I*) assessed by CatWalk analysis (% ipsilateral/contralateral). Data are expressed as mean ± SD. $^{***}P < 0.001$ *versus* the Scram group by two-way ANOVA followed by *post hoc* Bonferroni multiple comparison test, $F_{(1, 7)} = 17.85$ (*H*) and $F_{(1, 7)} = 93.15$ (*I*), n = 8 per group. (*J*) Combined paw print image. (*K*) Representative digitized paw prints and associated step cycles. PRDM1, positive regulatory domain I–binding factor 1.

$P < 0.001$; fig. 3H) and single stance (short hairpin RNA: 82.3 ± 17.4% *vs.* Scram: 29.8 ± 17.9%; two-way ANOVA; n = 8; $P < 0.0001$; fig. 3I). Representative images of the print area in the Scram and short hairpin RNA mouse groups are shown (fig. 3, J and K). We also repeated these experiments to verify the effect of PRDM1 knockdown in the dorsal root ganglion on the pain threshold and neuropathic pain hypersensitivity in female mice with similar results (Supplemental Digital Content 7, http://links.lww.com/ALN/C528).

To assess potential therapeutic effects of PRMD1 knockdown in treating established nociceptive response, we injected short hairpin RNA 7 days after the chronic constriction injury surgery. Our results show that chronic constriction injury–induced mechanical allodynia (fig. 4A), thermal hyperalgesia (fig. 4B), and cold hyperalgesia (fig. 4C) were relieved 2 weeks after dorsal root ganglion injection of PRDM1 short hairpin RNA. Furthermore, dorsal root ganglion injection of PRDM1 short hairpin RNA also reversed chronic constriction injury–induced decreased in the percentage of the print area (chronic constriction injury + short hairpin RNA: 68.0 ± 13.3% *vs.* chronic constriction injury + Scram: 22.8 ± 12.8%; two-way ANOVA; n = 8; $P < 0.0001$; fig. 4D) and single stance (chronic constriction injury + short hairpin RNA: 75.3 ± 15.6% *vs.* chronic constriction injury + Scram: 45.1 ± 15.1%; two-way ANOVA; n = 8; $P = 0.046$; fig. 4E). Representative images show the print area in the sham + Scram, chronic constriction injury + Scram, and chronic constriction injury + short hairpin RNA male mouse groups (fig. 4, F and G). Similar results were obtained in female mice (Supplemental Digital Content 8, http://links.lww.com/ALN/C529). Taken together, our results suggest that knockdown of PRDM1 can relieve hyperalgesia induced by peripheral nerve injury.

PRDM1 Knockdown Reduces Injured Dorsal Root Ganglion Neuronal Excitability

To determine whether PRDM1-dependent effects on nociceptive response in injured dorsal root ganglion neurons may be accounted for by an impact on neuronal excitability, we performed whole cell current clamp recordings on day 7 after chronic constriction injury, with assessment of the action potentials and resting membrane potential in ipsilateral lumbar 4 and lumbar 5 dorsal root ganglion neurons from mice injected with *Prdm1* short hairpin RNA or Scram. Compared with neurons in the Scram group, those in the *Prdm1* short hairpin RNA group showed a lower action potential firing rate in response to superimposed positive current injections ranging from 90 to 160 pA (fig. 5, A and B), but no difference was observed in action potential amplitude (fig. 5C). Furthermore, injection of *Prdm1* short hairpin RNA into the dorsal root ganglion hyperpolarized the resting membrane potential (chronic constriction injury + short hairpin RNA: −61.7 ± 11.4 mV *vs.* chronic constriction injury + Scram: −50.0 ± 10.5 mV; two-tailed unpaired *t* test, $t_{(53)} = 3.96$; n = 25 in the chronic constriction injury + short hairpin RNA group and n = 30 in the chronic constriction injury + Scram group; $P < 0.001$; fig. 5D) and increased the rheobase (chronic constriction injury + short hairpin RNA: 36.8 ± 25.1 pA *vs.* chronic constriction injury + Scram: 23.7 ± 15.0 pA; two-tailed unpaired *t* test, $t_{(53)} = 2.40$; n = 25 in the chronic constriction injury + short hairpin RNA group and n = 30 in the chronic constriction injury + Scram group; $P = 0.020$; fig. 5E) and action potential threshold (chronic constriction injury + short hairpin RNA: −28.9 ± 11.1 mV *vs.* chronic constriction injury + Scram: −16.5 ± 8.4 mV; two-tailed unpaired *t* test, $t_{(53)} = 4.68$; n = 25 in the chronic constriction injury + short hairpin RNA group and n = 30 in the chronic constriction injury + Scram group; $P < 0.0001$; fig. 5F). Collectively, these results suggest that endogenous PRDM1 regulates the excitability in injured dorsal root ganglion neurons, whereas abnormal firing of injured dorsal root ganglion neurons is normalized by PRDM1 knockdown.

Dorsal Root Ganglion PRDM1 Overexpression Leads to Pain Hypersensitivity

To further confirm that the increase in PRDM1 in the dorsal root ganglion at the early stage of nerve injury can indeed induce nociception, we injected adeno-associated virus 5 that expresses full-length *Prdm1* (adeno-associated virus 5–Prdm1) into the unilateral lumbar 4 and lumbar 5 dorsal root ganglions of naive mice. Adeno-associated virus 5–green fluorescent protein was used as a control. Four weeks after injection, the expression levels of *Prdm1* mRNA (fold change: PRDM1 overexpression: 5.2 ± 1.6 *vs.* green fluorescent protein: 1.0 ± 0.3; two-tailed unpaired *t* test, $t_{(10)} = 6.23$; n = 6; $P < 0.0001$; fig. 6A) and PRDM1 protein (fold change: PRDM1 overexpression: 2.5 ± 0.7 *vs.* green fluorescent protein: 1.0 ± 0.4; two-tailed unpaired *t* test, $t_{(6)} = 4.68$; n = 6; $P = 0.001$; fig. 6, B and C) in the dorsal root ganglion of adeno-associated virus 5–Prdm1–injected mice were higher than those in the dorsal root ganglion of adeno-associated virus 5–green fluorescent protein–injected mice. The overexpression of Flag-tagged PRDM1 was verified by Western blotting with an anti-Flag antibody (fig. 6D). Behavioral results showed that the paw withdrawal threshold to mechanical stimulation (PRDM1 overexpression: 0.6 ± 0.3 g *vs.* green fluorescent protein: 1.2 ± 0.2 g; two-way ANOVA; n = 13; $P < 0.0001$; fig. 6E) and paw withdrawal latency to thermal (PRDM1 overexpression: 5.2 ± 1.3 s *vs.* green fluorescent protein: 9.8 ± 1.7 s; two-way ANOVA; n = 13; $P < 0.0001$; fig. 6F) and cold (PRDM1 overexpression: 3.4 ± 0.5 s *vs.* green fluorescent protein: 5.3 ± 0.6 s; two-way ANOVA; n = 13; $P < 0.0001$; fig. 6G) stimulation of mice injected with adeno-associated virus 5–Prdm1 were lower than those of mice injected with adeno-associated virus 5–green fluorescent protein. Similar results were also observed in female mice (Supplemental Digital Content 9, http://links.lww.com/ALN/C530).

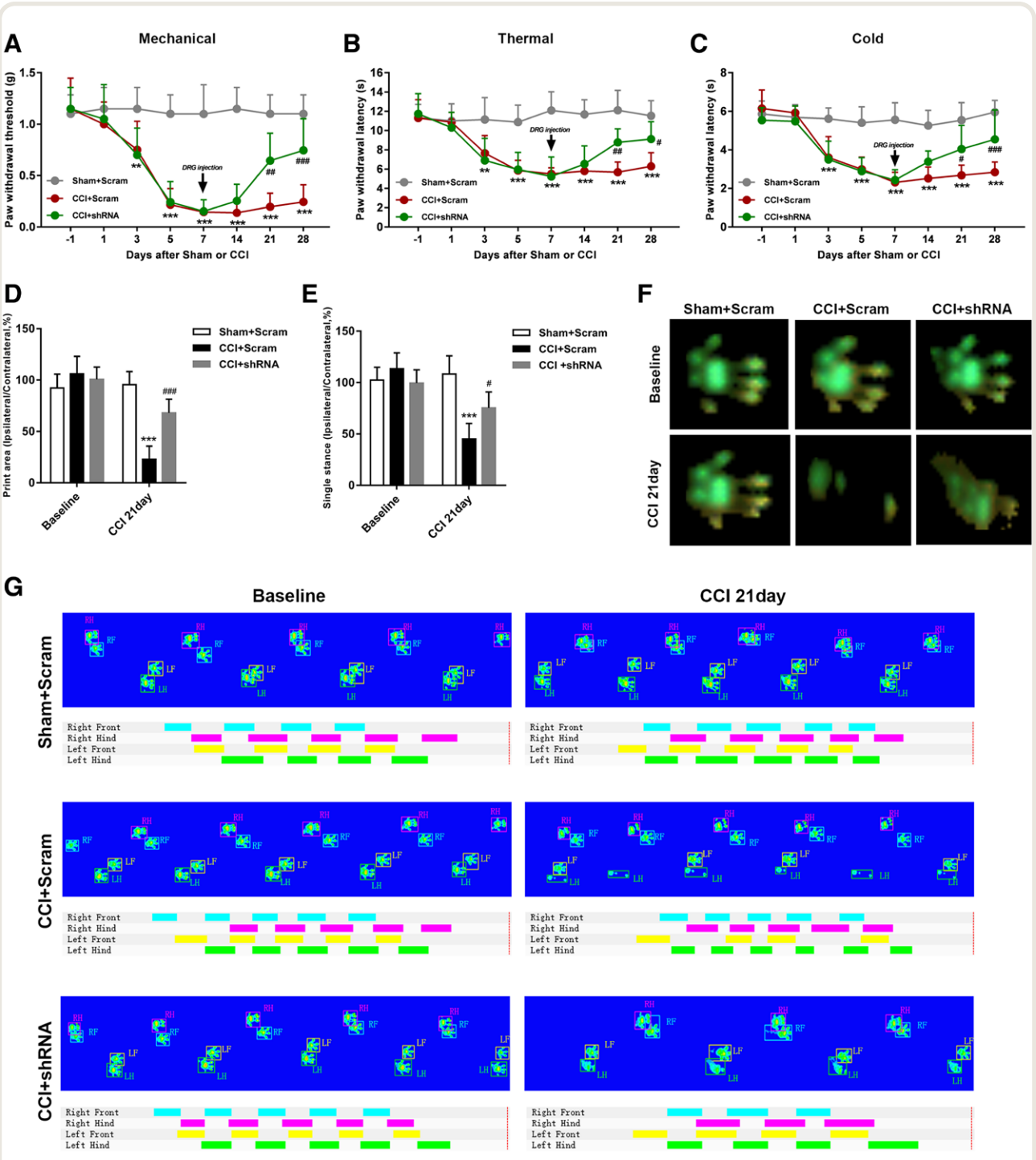

Fig. 4. Dorsal root ganglion knockdown of PRDM1 attenuates chronic constriction injury–induced hyperalgesia. (*A* through *C*) Dorsal root ganglion microinjection of short hairpin RNA attenuates chronic constriction injury–induced mechanical allodynia (*A*), thermal hyperalgesia (*B*), and cold hyperalgesia (*C*). Short hairpin RNA or Scram was injected on day 7 after chronic constriction injury. Data are expressed as mean ± SD. $^{**}P < 0.01$ and $^{***}P < 0.001$ *versus* the sham + Scram group; $\#P < 0.05$, $\#\#P < 0.01$, and $\#\#\#P < 0.001$ *versus* the chronic constriction injury + Scram group by two-way ANOVA followed by *post hoc* Bonferroni multiple comparison test, $F_{(14, 168)} = 10.10$ (*A*), $F_{(14, 168)} = 7.19$ (*B*), and $F_{(14, 168)} = 8.08$ (*C*), n = 8 per group. (*D* and *E*) Dorsal root ganglion microinjection of short hairpin RNA attenuates chronic constriction injury–induced decrease in paw print area (*D*) and single stance (*E*). Data are expressed as mean ± SD. $^{***}P < 0.001$ *versus* the sham + Scram group; $\#P < 0.05$ and $\#\#\# P < 0.001$ *versus* the chronic constriction injury + Scram group by two-way ANOVA followed by *post hoc* Bonferroni multiple comparison test, $F_{(2, 14)} = 47.12$ (*D*) and $F_{(2, 14)} = 14.78$ (*E*), n = 8 per group. (*F*) Combined paw print image. (*G*) Representative digitized paw prints and associated step cycles. PRDM1, positive regulatory domain I–binding factor 1.

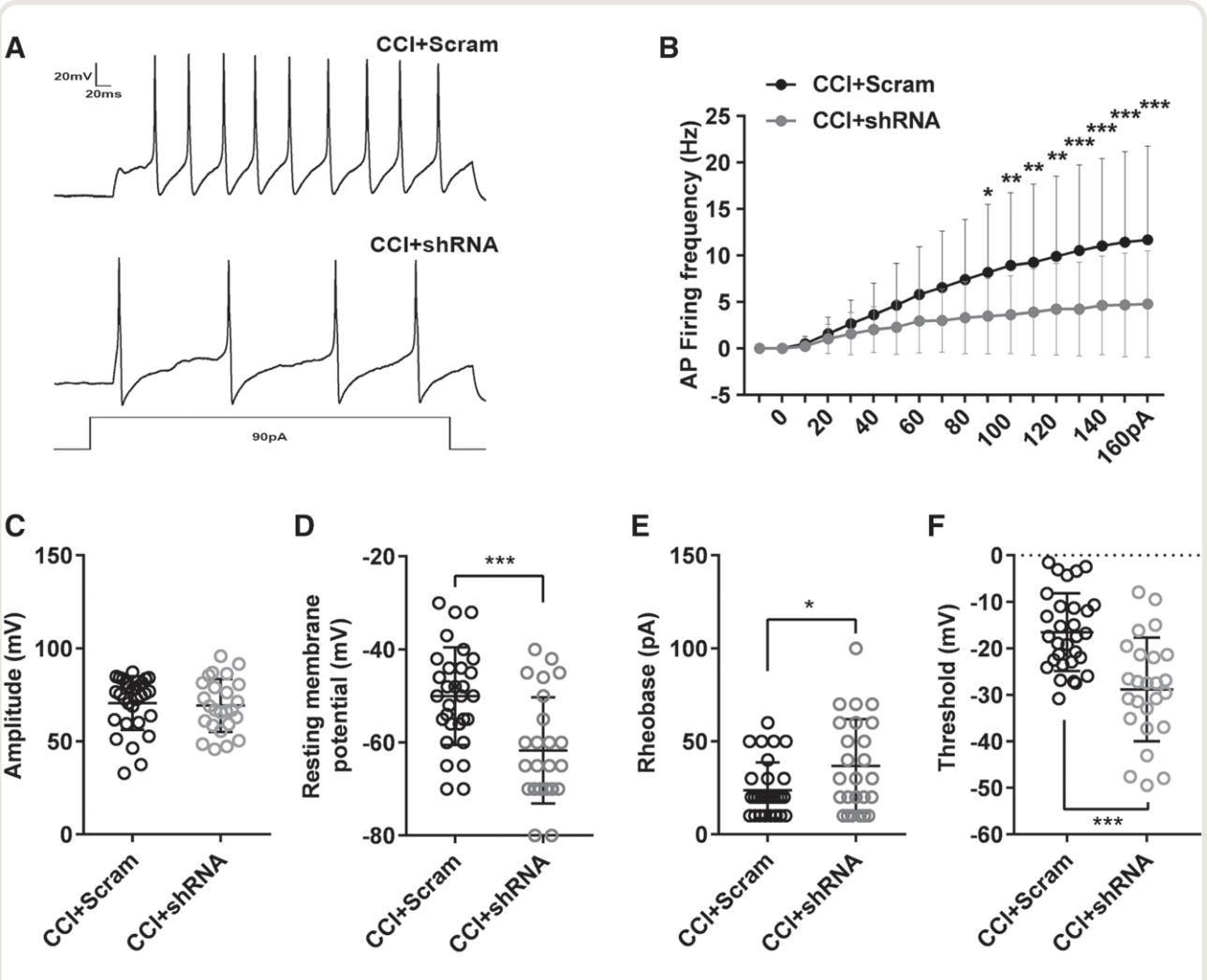

Fig. 5. Specific downregulation of PRDM1 alters the excitability of dorsal root ganglion neurons from chronic constriction injury mice. (*A*) Current clamp recordings of action potential traces in dorsal root ganglion green fluorescent protein–positive neurons on day 7 after chronic constriction injury from short hairpin RNA– and Scram-injected mice. (*B*) Quantification of action potential firing frequency in dorsal root ganglion green fluorescent protein–positive neurons of short hairpin RNA– and Scram-injected chronic constriction injury mice. Data are expressed as mean ± SD. **P* < 0.05, ***P* < 0.01, and ****P* < 0.001 *versus* the chronic constriction injury + Scram group by two-way ANOVA followed by *post hoc* Bonferroni test, $F_{(17, 1025)} = 2.68$, n = 25 in the chronic constriction injury + short hairpin RNA group and n = 30 in the chronic constriction injury + Scram group. (*C* through *F*) Quantification of amplitude (*C*), resting membrane potential (*D*), rheobase (*E*), and threshold of action potential generation (*F*) in dorsal root ganglion green fluorescent protein–positive neurons of short hairpin RNA– and Scram-injected chronic constriction injury mice. Data are expressed as mean ± SD. **P* < 0.05 and ***P* < 0.01 *versus* the chronic constriction injury + Scram group by unpaired *t* test, n = 25 in the chronic constriction injury + short hairpin RNA group and n = 30 in the chronic constriction injury + Scram group. PRDM1, positive regulatory domain I–binding factor 1.

These findings indicate that overexpression of PRDM1 in the dorsal root ganglion of naive mice leads to mechanical allodynia and thermal and cold hyperalgesia, which are similar to nociception symptoms.

PRDM1 Represses Kv4.3 Channel Expression in Dorsal Root Ganglion Neurons

To identify genes that may be regulated by PRDM1 in the injured dorsal root ganglion after chronic constriction injury, we performed RNA sequencing analysis on injured dorsal root ganglions from short hairpin RNA– and Scram-injected mice. The scatter plot shows the differentially expressed genes (fig. 7A), and the differentially expressed gene heat map depicts their hierarchical clustering (fig. 7B). Among the differentially expressed genes, *Cacna1g* ($Ca_V3.1$),[25] Cxcl5,[26] Cxcl12,[27] *Cxcr2*,[28] *Ednra*,[29,30] *Htr2b* ($5\text{-}HT_{2B}$),[31] *Kcnj2* (Kir2.1),[32] *Mmp9*,[33] and *Prkcg* (PKCγ)[34,35] are classically involved in peripheral sensitization of neuropathic pain (table 1). The identification of

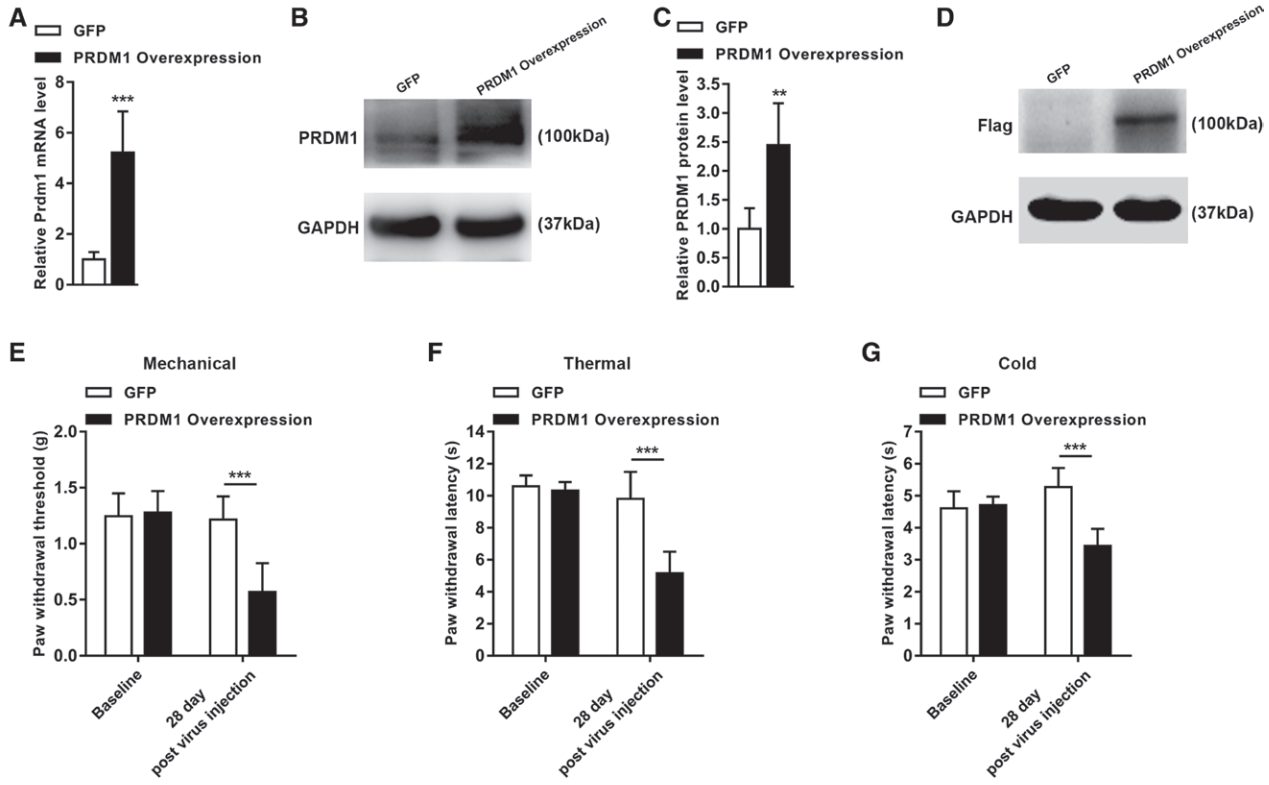

Fig. 6. PRDM1 overexpression in sensory neurons of the dorsal root ganglion evokes hyperalgesia symptoms in naive mice. (*A*) Level of *Prdm1* mRNA in ipsilateral lumbar 4 and lumbar 5 dorsal root ganglions after microinjection of adeno-associated virus 5–Prdm1–overexpressing virus (PRDM1 overexpression) and adeno-associated virus 5–green fluorescent protein control virus into the unilateral lumbar 4 and lumbar 5 dorsal root ganglions in mice. Data are expressed as mean ± SD. ***$P < 0.001$ *versus* the green fluorescent protein group by two-tailed unpaired *t* test, n = 6 per group. (*B* and *C*) Levels of PRDM1 protein in ipsilateral lumbar 4 and lumbar 5 dorsal root ganglions after microinjection of PRDM1 overexpression and green fluorescent protein into unilateral lumbar 4 and lumbar 5 dorsal root ganglions in mice. Data are expressed as mean ± SD. **$P < 0.01$ *versus* the green fluorescent protein group by two-tailed unpaired *t* test, n = 6 per group. (*D*) Dorsal root ganglions were infected with Flag-PRDM1 and subjected to Western blot using the Flag antibody. (*E* through *G*) Paw withdrawal responses to mechanical (*E*), thermal (*F*), and cold (*G*) stimuli on the ipsilateral side after microinjection of PRDM1 overexpression and green fluorescent protein virus into ipsilateral lumbar 4 and lumbar 5 dorsal root ganglions in naive mice. Data are expressed as mean ± SD. ***$P < 0.001$ *versus* the green fluorescent protein group by two-way ANOVA followed by *post hoc* Bonferroni multiple comparison test, $F_{(1, 48)} = 31.91$ (*E*), $F_{(1, 48)} = 46.43$ (*F*), and $F_{(1, 48)} = 48.89$ (*G*), n = 13 per group. PRDM1, positive regulatory domain I–binding factor 1.

differentially expressed genes by RNA sequencing was confirmed by reverse transcription quantitative polymerase chain reaction, for which we selected seven differentially expressed genes for validation (fig. 7, C through I). Among these differentially expressed genes, only *Kcnd3* was upregulated after PRDM1 knockdown. This gene encodes Kv4.3, a member of the A-type voltage-gated K^+ channel family that is selectively expressed in nociceptive dorsal root ganglion neurons and is inversely associated with the development of chronic pain.[36,37] Suppression of *Kcnd3* expression by PRDM1 in injured dorsal root ganglions might contribute to the function of PRDM1 in promoting neuron excitability and nociceptive response. Because PRDM1 acts as a transcriptional repressor, the downregulation of the other genes may be associated with decreased peripheral sensitization after PRDM1 knockdown rather than direct suppression by PRDM1.

To verify a role of Kv4.3 in mediating PRDM1-dependent peripheral nerve injury–induced nociception in the dorsal root ganglion, we evaluated Kv4.3 protein expression after PRDM1 knockdown. Injection of *Prdm1* short hairpin RNA but not Scram increased the basal expression level of Kv4.3 protein in lumbar 4 and lumbar 5 dorsal root ganglions of sham-operated mice (fold change: sham + short hairpin RNA: 1.5 ± 0.5 *vs.* sham + Scram: 1.0 ± 0.2; one-way ANOVA; n = 6; $P = 0.026$) and statistically reversed the decrease in Kv4.3 protein expression on day 7 after chronic constriction injury in injured dorsal root ganglions (fold change: chronic constriction injury + short hairpin RNA: 1.2 ± 0.3 *vs.* chronic constriction

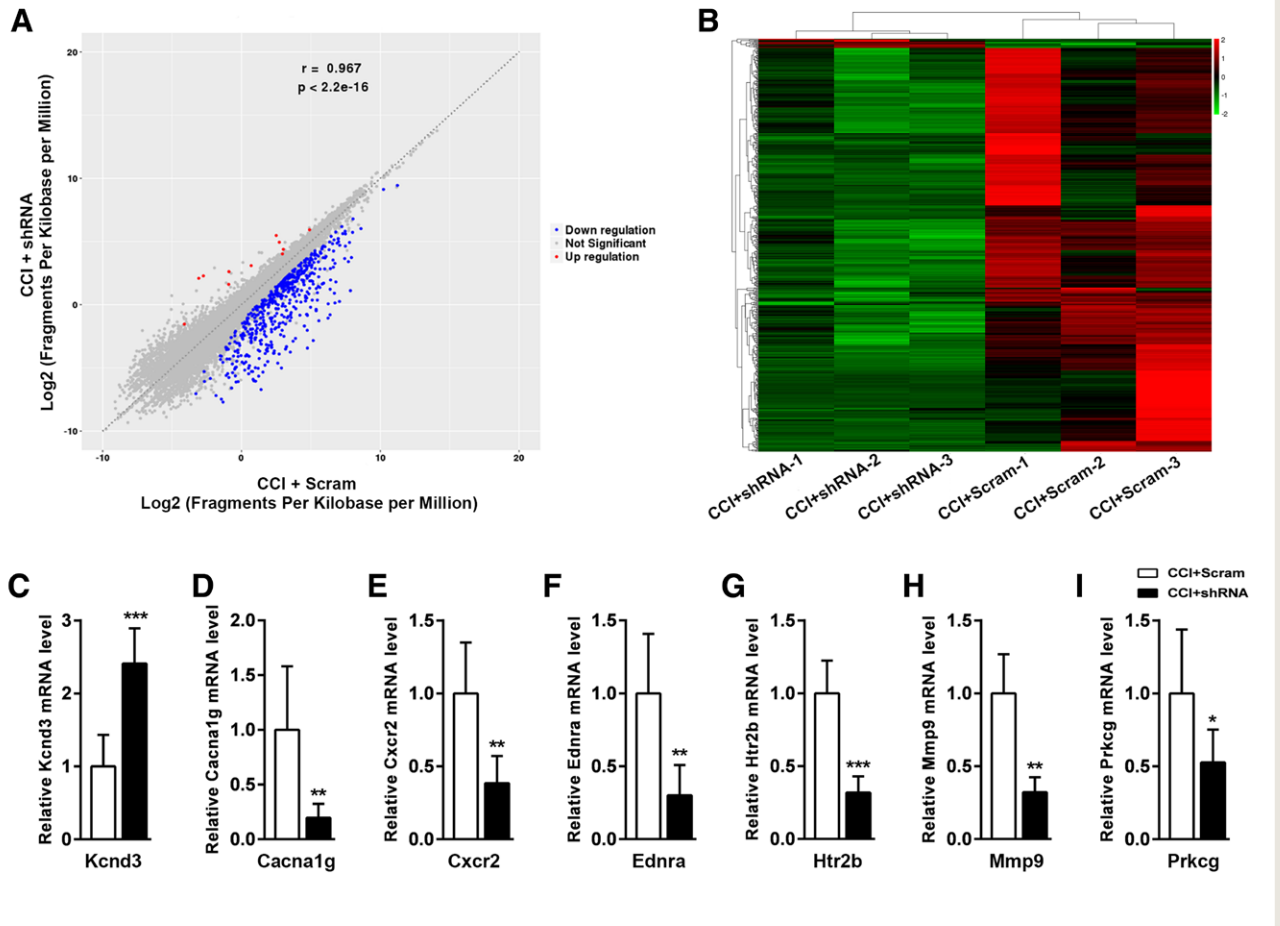

Fig. 7. Differentially expressed genes in the dorsal root ganglion of chronic constriction injury mice with or without PRDM1 knockdown determined by RNA sequencing technology. (*A*) Scatter plot showing the upregulated and downregulated genes in ipsilateral lumbar 4 and lumbar 5 dorsal root ganglions in the chronic constriction injury + short hairpin RNA group compared with the chronic constriction injury + Scram group. *Red dots* represent genes with statistically significant upregulation of expression, *blue dots* represent genes with statistically significant downregulation of expression, and *gray dots* represent genes with no significant difference. (*B*) Heat map showing hierarchical clustering of differentially expressed genes of mice in the chronic constriction injury + short hairpin RNA group compared with the chronic constriction injury + Scram group. Upregulated and downregulated genes are colored in *red* and *green*, respectively. (*C* through *I*) Seven differentially expressed genes identified by RNA sequencing (shown in table 1) and verified by quantitative polymerase chain. Data are expressed as mean ± SD. *$P < 0.05$, **$P < 0.01$, and ***$P < 0.001$ *versus* chronic constriction injury + Scram group by two-tailed unpaired *t* test, n = 6 per group. PRDM1, positive regulatory domain I–binding factor 1.

injury + Scram: 0.4 ± 0.1; one-way ANOVA; n = 6; $P = 0.003$; fig. 8, A and B). Furthermore, overexpression of PRDM1 through injection of *Prdm1*-overexpressing virus into the dorsal root ganglion of naive mice reduced the levels of *Kcnd3* mRNA (fold change: PRDM1 overexpression: 0.4 ± 0.2 *vs.* green fluorescent protein: 1.0 ± 0.3; two-tailed unpaired *t* test, $t_{(10)} = 4.39$; n = 6; $P = 0.001$; fig. 8C) and Kv4.3 protein (fold change: PRDM1 overexpression: 0.4 ± 0.1 *vs.* green fluorescent protein: 1.0 ± 0.3; two-tailed unpaired *t* test, $t_{(6)} = 2.98$; n = 6; $P < 0.001$; fig. 8, D and E). These data strongly suggest that PRDM1 is involved in downregulation of the Kv4.3 channel after peripheral nerve injury.

To test whether the *Kcnd3* gene is a direct target of PRDM1, we performed site-directed chromatin immunoprecipitation–quantitative polymerase chain reaction assays with an antibody specific for PRDM1 at five different regions of the *Kcnd3* gene locus (fig. 8F). The PRDM1-binding activity of two regions (R3 and R4) of the *Kcnd3* gene in the injured dorsal root ganglion was higher in the chronic constriction injury group than in the sham group on day 7 after chronic constriction injury (fig. 8G). Thus, these results are consistent with the possibility that PRDM1 transcriptionally represses the *Kcnd3* gene in the injured dorsal root ganglion *via* enhanced binding to the *Kcnd3* gene promoter region.

Table 1. The Nociceptive Response–related Differentially Expressed Genes in the Ipsilateral Lumbar 4 and Lumbar 5 Dorsal Root Ganglions of the Chronic Constriction Injury + Short Hairpin RNA Group Compared with the Chronic Constriction Injury + Scram Group

Gene Name	Chronic Constriction Injury + Scram (Fragments per Kilobase per Million)	Chronic Constriction Injury + Short Hairpin RNA (Fragments per Kilobase per Million)	Fold Change	*P* Value	UP/DOWN
Kcnd3	1.62	8.50	2.39	< 0.001	UP
Cacna1g	1.27	0.36	−1.82	< 0.001	DOWN
Cxcl12	19.66	5.41	−1.86	= 0.001	DOWN
Cxcl5	3.65	0.09	−5.31	< 0.001	DOWN
Cxcr2	1.21	0.28	−2.11	< 0.001	DOWN
Ednra	6.09	2.73	−1.16	< 0.001	DOWN
Htr2b	3.13	0.20	−4.00	< 0.001	DOWN
Kcnj2	8.19	2.88	−1.51	< 0.001	DOWN
Mmp9	10.67	2.17	−2.30	< 0.001	DOWN
Prkcg	0.72	0.22	−1.73	= 0.001	DOWN

PRDM1 Knockdown in the Dorsal Root Ganglion Reduces the Response of Spinal Dorsal Horn Neurons to Peripheral Nociceptive Stimuli

To directly visualize spinal dorsal horn neuron responses after dorsal root ganglion PRDM1 knockdown, we performed *in vivo* two-photon imaging of thermal stimuli–evoked calcium signals in spinal dorsal horn neurons in mice. GCaMP6s virus was injected into the spinal cord at the level of the lumbar 4–lumbar 5 dorsal horn (fig. 9A), and the transfection efficiency was verified by GCaMP6s labeling using immunohistochemistry with a green fluorescent protein antibody 4 weeks after injection (fig. 9B). We used tissue clearing technology to make the spinal cord transparent and then performed three-dimensional image reconstruction processing to clearly observe the expression of the GCaMP6s virus in the spinal dorsal horn (Supplemental Digital Content 10, http://links.lww.com/ALN/C531). Stable images were achieved by using a custom clamp to hold the spinous process (fig. 9C), and consistent labeling of green fluorescent protein was detected in the lumbar 4–lumbar 5 spinal dorsal horn.

Because temperature-sensing dorsal root ganglion neurons are mainly projected to the superficial laminae of spinal dorsal horn neurons, we focused on the changes in calcium signals in neurons less than 200 μm below the surface of the spinal cord. We examined the response to thermal pain hypersensitivity stimulation (target temperature: 45°C; maintained for 10 s) and observed robust, reliable calcium transients in subsets of spinal dorsal horn neurons in control Scram-treated mice (fig. 9, D and F; Supplemental Digital Content 11, Movie S3, http://links.lww.com/ALN/C532). However, we observed a decrease in the number of neurons specifically activated by thermal stimulation in *Prdm1* short hairpin RNA–treated mice (fig. 9, E and F; Supplemental Digital Content 12, Movie S4, http://links.lww.com/ALN/C533). Furthermore, the peak response amplitudes of the short hairpin RNA group were lower than those of the Scram group (Δfluorescence/fluorescence: naive + short hairpin RNA: 84.6 ± 19.8% *vs.* naive + Scram: 210 ± 58.3%; two-tailed unpaired *t* test, $t_{(154)} = 17.73$; n = 76 cells in naive + short hairpin RNA group and n = 80 cells in naive + Scram group; $P < 0.0001$; fig. 9G). Together, these results confirm the important role of PRDM1 in the dorsal root ganglion in the perception of peripheral nociceptive stimuli.

Discussion

Our study reveals the alteration and functional significance of PRDM1 in a peripheral nerve injury–induced nociception animal model. The principle findings are fourfold: (1) peripheral nerve injury leads to an increase in PRDM1 expression in injured dorsal root ganglion neurons; (2) this increase is associated with the downregulation of Kv4.3 channel expression in injured dorsal root ganglion neurons caused by peripheral nerve injury; (3) blocking the increase in PRDM1 restores Kv4.3 channel expression, reduces the hyperexcitability of injured dorsal root ganglion neurons, and attenuates peripheral nerve injury–induced nociception; (4) PRDM1 overexpression in naive mouse dorsal root ganglion neurons diminishes Kv4.3 channel expression and induces hyperalgesia. Because Kv4.3 channel downregulation contributes to nociception genesis,[3,38] PRDM1, as a transcriptional suppressor, likely participates in peripheral nerve injury–induced nociception genesis by repressing Kv4.3 channel expression in the injured dorsal root ganglion.

PRDM1 is a member of the PRDI-BF1 and RIZ homology domain–containing protein family, which contains 16 to 17 family members in mammals. PRDM1 was first identified as a repressor of interferon-β gene expression[6] but was later discovered to be required for the differentiation of mature B lymphocytes into plasma cells.[39] Recently, PRDM1 has also been shown to participate in certain biologic processes in the nervous system. For example, PRDM1 is expressed in both mesodermal cells and neural plates involved in nervous system development.

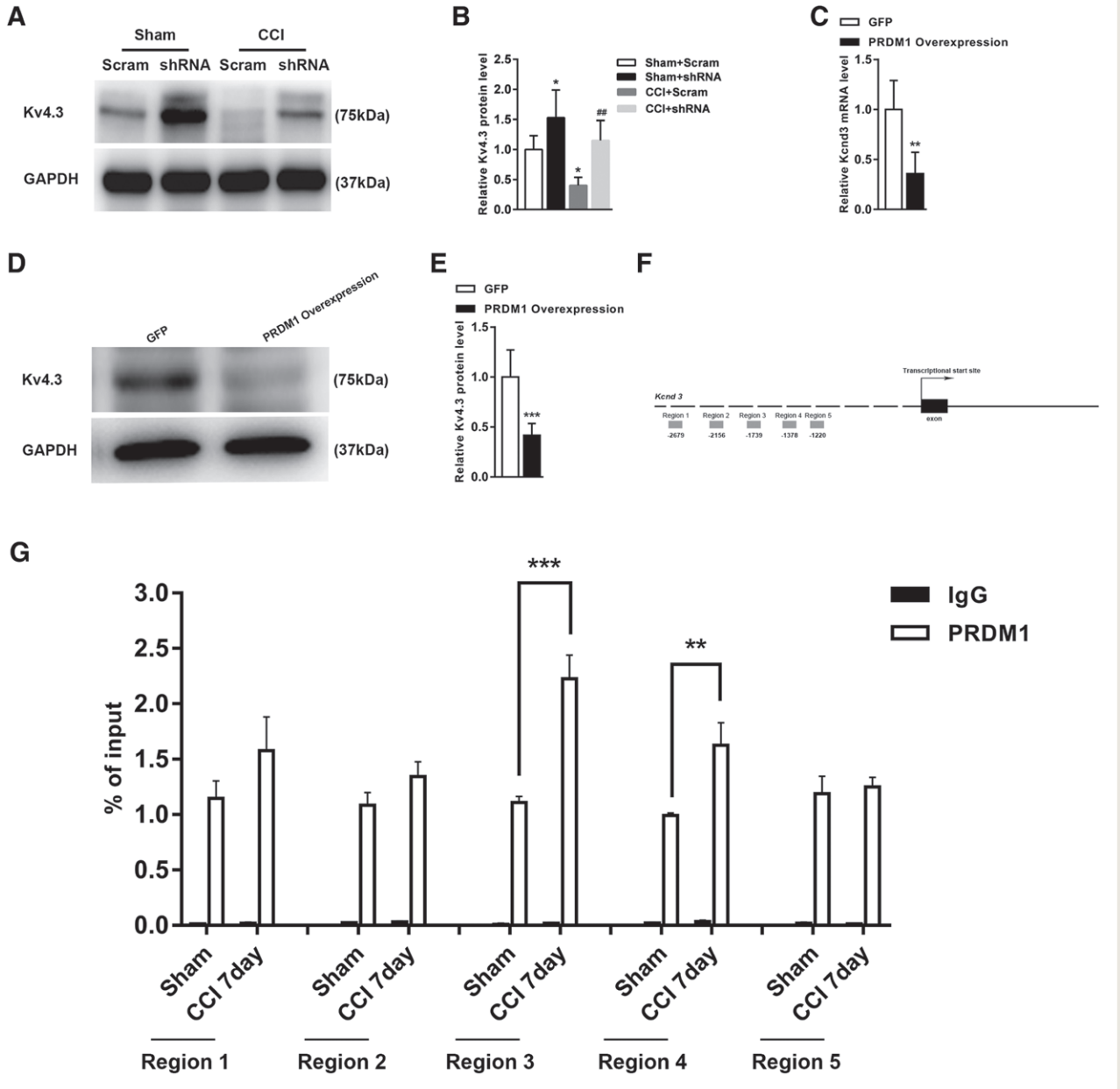

Fig. 8. PRDM1 represses the expression of the Kv4.3 channel in dorsal root ganglion neurons. (*A* and *B*) Levels of Kv4.3 protein in ipsilateral lumbar 4 and lumbar 5 dorsal root ganglions on day 7 after chronic constriction injury or sham surgery from short hairpin RNA– or Scram-injected mice. Data are expressed as mean ± SD. *$P < 0.05$ *versus* the corresponding sham + Scram group, ##$P < 0.01$ *versus* the corresponding chronic constriction injury + Scram group. One-way ANOVA followed by *post hoc* Tukey test, $F_{(3, 20)} = 13.33$, n = 6 per group. (*C*) Level of *Kcnd3* mRNA in ipsilateral lumbar 4 and lumbar 5 dorsal root ganglions after microinjection of PRDM1 overexpression and green fluorescent protein into unilateral lumbar 4 and lumbar 5 dorsal root ganglions in mice. Data are expressed as mean ± SD. ** $P < 0.01$ *versus* the green fluorescent protein group by two-tailed unpaired *t* test, n = 6 per group. (*D* and *E*) Levels of Kv4.3 protein in ipsilateral lumbar 4 and lumbar 5 dorsal root ganglions after microinjection of PRDM1 overexpression and green fluorescent protein into unilateral lumbar 4 and lumbar 5 dorsal root ganglions in mice. Data are expressed as mean ± SD. ***$P < 0.001$ *versus* the green fluorescent protein group by two-tailed unpaired *t* test, n = 6 per group. (*F*) Schematic diagram of the *Kcnd3* gene with the exon depicted as a black box. Primers for chromatin immunoprecipitation–quantitative polymerase chain experiments are shown as *gray rectangles*. (*G*) Chromatin from sham and injured dorsal root ganglions 7 days after chronic constriction injury was immunoprecipitated with an antibody specific for PRDM1 or immunoglobulin G as a negative control, followed by quantitative polymerase chain with primers specific for five different regions of the *Kcnd3* gene, as illustrated in panel *F*. Data are expressed as mean ± SD. **$P < 0.01$, ***$P < 0.001$ *versus* the sham group by two-tailed unpaired *t* test, n = 3 repeats per group. Note that in most cases, the immunoglobulin G negative control has a very low percentage of input levels and is therefore not visible in most of the graphs. PRDM1, positive regulatory domain I–binding factor 1.

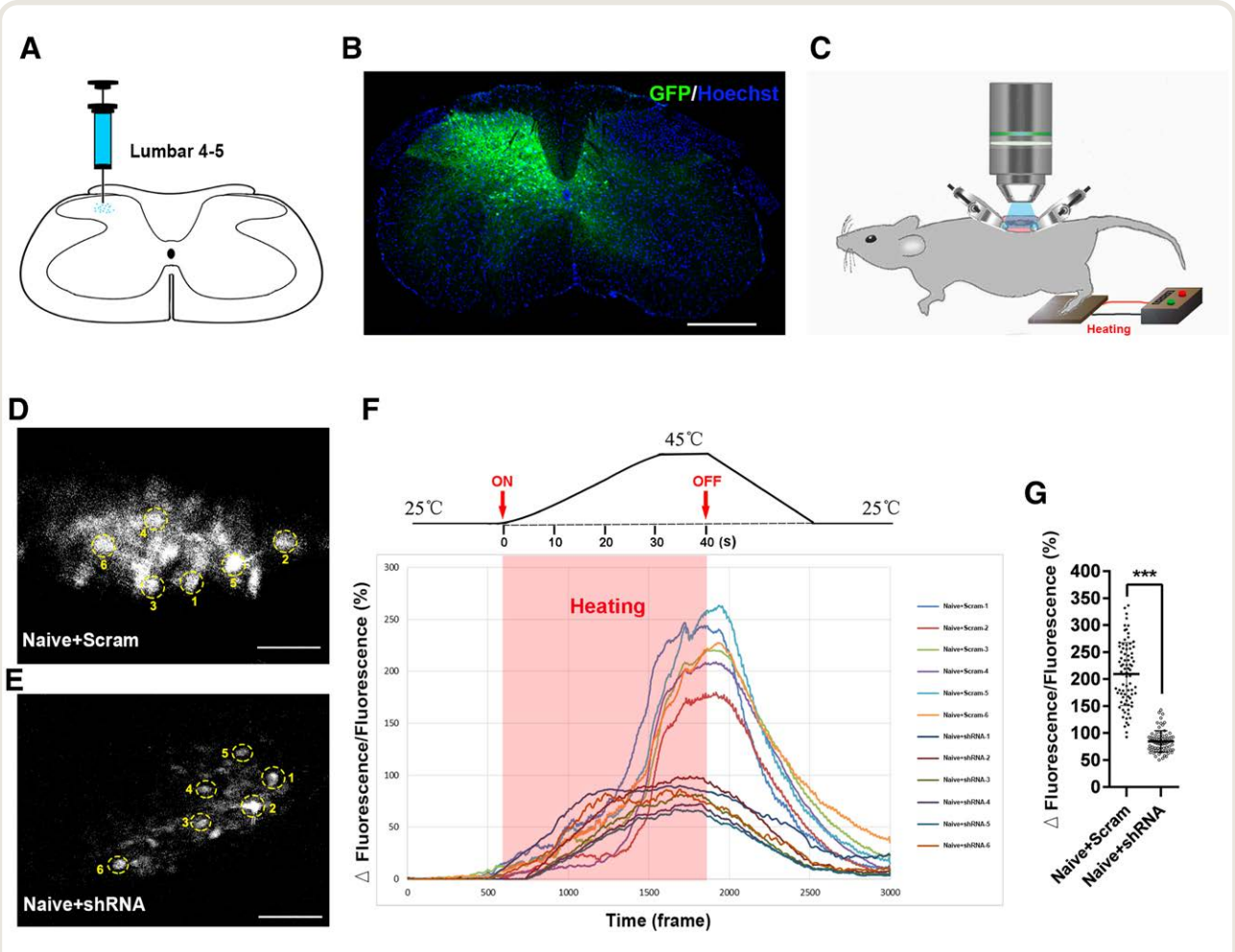

Fig. 9. *In vivo* two-photon calcium imaging in the spinal cord after PRDM1 knockdown in the dorsal root ganglion. (*A*) Illustration of the injection of GCaMP6s into the spinal dorsal horn of dorsal root ganglion PRDM1 knockdown mice. (*B*) Representative image of GCaMP6s-positive cells in the ipsilateral spinal dorsal horn after adeno-associated virus 5–human synapsin–GCaMP6s injection. *Scale bar*, 400 μm. (*C*) Schematic illustrating the imaging preparation. The mouse was fixed by attaching custom-made clamps to the vertebral column. (*D* through *F*) Heating-evoked calcium transients in subsets of superficial dorsal horn cells *in vivo*. Two-photon image showing GCaMP6s-labeled neuronal populations in the ipsilateral superficial dorsal horn in the naive + Scram group (*D*) and naive + short hairpin RNA group (*E*). *Scale bar*, 100 μm. *Yellow circles* indicate regions of interest for which the corresponding fluorescence traces (Δfluorescence/fluorescence) are shown on the right (*F*). (*G*) The peak Δfluorescence/fluorescence amplitudes of fluorescence transients from short hairpin RNA– (n = 76; cells) or Scram-injected mice (n = 80; cells). Data are expressed as mean ± SD. ***$P < 0.001$ *versus* the naive + Scram group by two-tailed unpaired *t* test. PRDM1, positive regulatory domain I–binding factor 1.

Knockout of PRDM1 in zebrafish leads to a loss of neural crest cells and Rohon–Beard sensory neurons, which ultimately leads to abnormal peripheral nervous system development.[10] The *sox*10 gene is a primary effector of PRDM1 in the neural crest, and *islet1* lies downstream of PRDM1 in the development of Rohon–Beard sensory neurons. PRDM1 is widely expressed in most tissues, including the nervous system, with expression reported in the dorsal root ganglion in mice.[11] However, the distribution pattern of PRDM1 in the mouse dorsal root ganglion was not clear before this study. We detected PRDM1 in the nuclei of dorsal root ganglion neurons but not in satellite cells. Furthermore, we revealed that PRDM1 is expressed in calcitonin gene–related peptide–, isolectin B4–, and neurofilament-200–labeled neurons, suggesting that PRDM1 is mainly distributed in medium- and small-sized nociceptive dorsal root ganglion neurons. We demonstrated activation of the PRDM1 gene in the dorsal root ganglion at the transcriptional level, with increased expression of PRDM1 mRNA and protein in the dorsal root ganglion after peripheral nerve injury. PRDM1 upregulation occurred at the onset of behaviorally expressed pain hypersensitivity and persisted for 7 days after peripheral nerve injury. These findings suggest that PRDM1 may function in peripheral

nociceptive transmission in the early period after peripheral nerve injury. Consistent with this possibility, injection of *Prdm1* short hairpin RNA into mouse dorsal root ganglions specifically blocked the peripheral nerve injury–induced increase in PRDM1 and attenuated nociception. Notably, our findings are also supported by a recent clinical report that reveals that PRDM12 (a member of the PRDI-BF1 and RIZ homology domain–containing family) is essential for human perception of pain, as pathogenic mutations cause a congenital loss of pain perception in humans.[40] This clinical finding further indicates that the PRDI-BF1 and RIZ homology domain–containing family may play a role in pain perception and provides clinical support for our study.

Peripheral nerve injury can cause the upregulation or downregulation of many dorsal root ganglion genes, including those involved in inflammatory responses,[41] G protein–coupled receptors,[31] neurotrophins,[42] and ion channels.[25] Strikingly, our RNA sequencing data showed that knockdown of PRDM1 restored the expression of the Kv4.3 channel gene in injured dorsal root ganglions. The Kv4.3 channel belongs to a family of voltage-gated K^+ channels that can be activated transiently and inactivated rapidly.[43] Many voltage-gated K^+ channels contribute to the regulation of dorsal root ganglion neuron excitability and pain hypersensitivity.[38] Peripheral nerve injury results in the downregulation of voltage-gated K^+ channel gene expression, reduction in outward voltage-gated K^+ currents, increased abnormal excitability, and ectopic spontaneous discharge of primary sensory neurons in the dorsal root ganglion, all of which may increase pain hypersensitivity.[4,44] We observed a decrease in Kv4.3 channel expression within 7 days after peripheral nerve injury, which is consistent with a previous report.[4] A previous study has reported that in the absence of pain stimulation, *Prdm1* expression is low and Kv4.3 expression is much higher in sensory neurons of the dorsal root ganglion.[45] Therefore, there is little overlap in the expression of these two proteins. As shown in the current work, PRDM1 expression is dependent on the pain level. Although reverse coupling of PRDM1 expression with Kv4.3 can lead to the detection of either *Prdm1* or Kv4.3 transcripts under certain conditions, these proteins are not usually coexpressed.[45] However, we cannot rule out that the repression of Kv4.3 in response to nociceptive pain may involve the coordinate function of additional corepressors. Although numerous studies have reported changes in voltage-gated K^+ gene expression or current changes after peripheral nerve injury, whether these transcriptional changes serve to initiate and maintain peripheral nerve injury–induced voltage-gated K^+ channel gene decrease in chronic pain remained unresolved before this study. Our results demonstrate that knockdown of PRDM1 restores Kv4.3 channel expression in the injured dorsal root ganglion, whereas mimicking the chronic constriction injury–induced increase in dorsal root ganglion PRDM1 *via* genetic overexpression decreases the expression of the Kv4.3 channel. These findings suggest that PRDM1 may negatively regulate Kv4.3 channel expression in the dorsal root ganglion after chronic constriction injury. PRDM1, as a transcriptional repressor, modulates the expression of many genes by directly binding DNA or acting as a scaffold to recruit multiple corepressor proteins, such as G9a[6] and histone deacetylase.[5] However, peripheral nerve injury–induced gene expression changes likely involve multiple transcriptional regulators, and we therefore performed chromatin immunoprecipitation–quantitative polymerase chain reaction to determine whether PRDM1 regulation of Kv4.3 channel gene expression in peripheral nerve injury–induced nociception may involve direct interaction of PRDM1 at the *Kcnd3* gene promoter. Consistent with this possibility, chronic constriction injury increased the occupancy of PRDM1 at the *Kcnd3* promoter in injured dorsal root ganglion. Thus, our data provide evidence for the essential role of PRDM1-mediated inhibition of Kv4.3 channel gene expression in dorsal root ganglion neurons in peripheral nerve injury–induced nociception through direct transcriptional repression. Although PRDM1 is generally known for mediating transcriptional repression, our RNA sequencing data revealed that PRDM1 knockdown also normalizes the expression of many upregulated genes in the injured dorsal root ganglion, such as *Cacna1g*, *Cxcl12*, and *Ednra*. The downregulation of these genes in PRDM1 knockdown dorsal root ganglions could potentially be explained by a decrease in peripheral sensitization upon restoration of Kv4.3 channel expression.

Hyperexcitability of dorsal root ganglion neurons is a common phenomenon in various peripheral nerve injury–induced nociception animal models and is often associated with a reduction in K^+ currents. Among the affected K^+ channels, voltage-gated K^+ channels, which are protein complexes composed of ion-conducting integral protein α subunits and auxiliary cytoplasmic β subunits, play an important role in setting the resting membrane potential and controlling action potential repolarization and frequency.[4] We demonstrated that knockdown of PRDM1 normalizes abnormal firing of injured dorsal root ganglion neurons, indicating that PRDM1 knockdown reduces spontaneous depolarization of the membrane in dorsal root ganglion neurons upon restoration of Kv4.3 channel expression. Peripheral nociceptive information is transmitted to the dorsal horn of the spinal cord through dorsal root ganglion transformation, resulting in increased responsiveness of dorsal horn neurons.[41] Therefore, we assessed spinal dorsal horn neuron responses by recording calcium responses to heat stimuli in Scram-injected and PRDM1 short hairpin RNA–injected mice. Our data reveal that PRDM1 knockdown in the dorsal root ganglion also reduces the response of spinal dorsal horn neurons to peripheral nociceptive stimuli, potentially because of a decrease in the excitatory input of primary nociceptive neurons in the dorsal root ganglion.

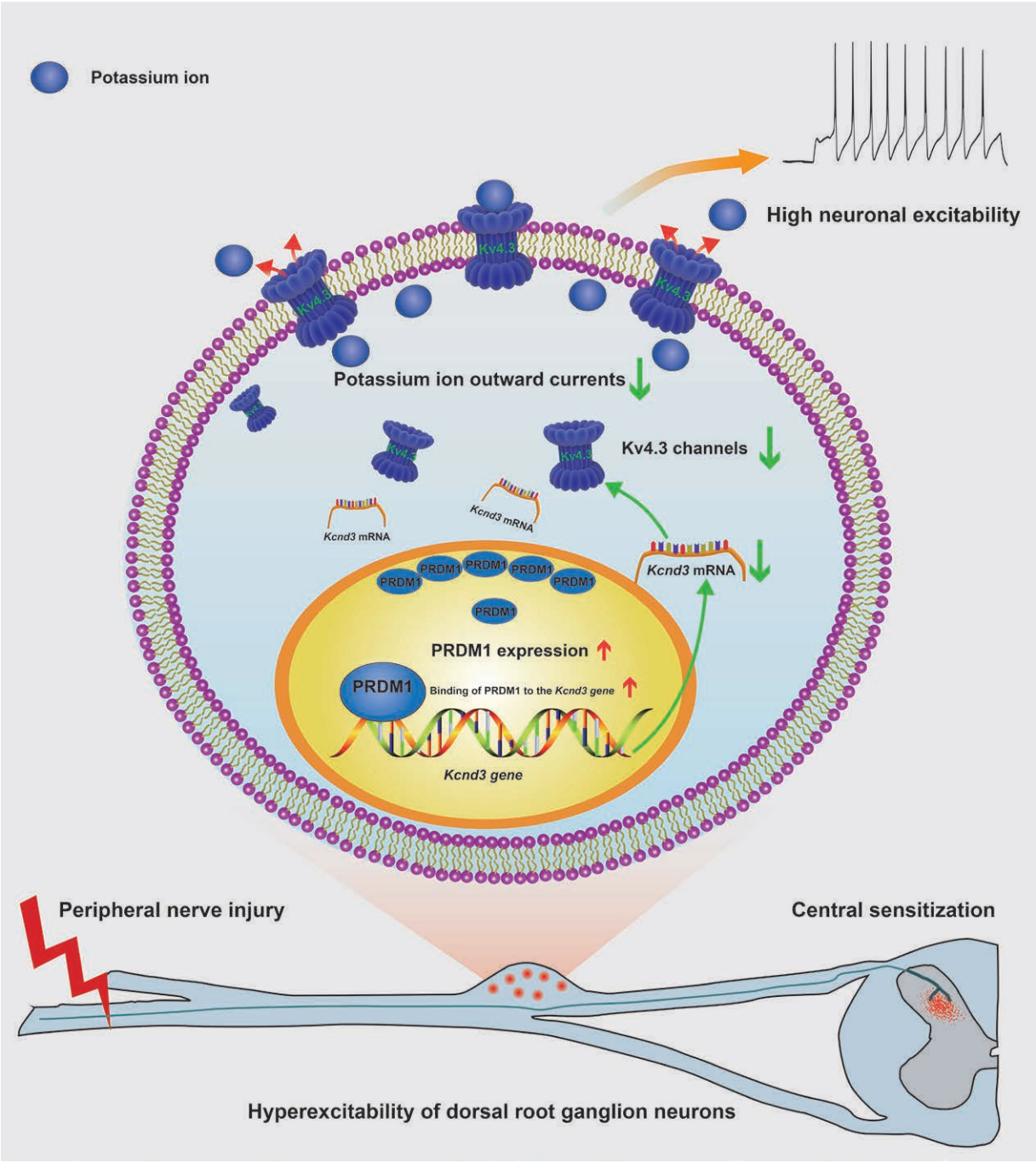

Fig. 10. Putative model for elucidating the relationship between peripheral nerve injury–induced nociception and the alteration of PRDM1 as well as the mechanism by which PRDM1 modulates Kv4.3 channels. With nociception development, PRDM1 expression in dorsal root ganglion neurons is increased, which can initiate transcriptional repression of the *Kcnd3* gene. Our results indicate that PRDM1-mediated *Kcnd3* gene silencing can be accomplished by PRDM1 binding directly to the DNA promoter region to initiate transcriptional repression. This transcriptional repression leads to decreased *Kcnd3* mRNA expression, fewer Kv4.3 ion channels, and ultimately decreased outward potassium current, increased dorsal root ganglion neuronal excitability, and sensitized neurons in the spinal dorsal horn. PRDM1, positive regulatory domain I–binding factor 1.

In summary, our study reveals that the transcriptional repressor PRDM1 triggers Kv4.3 channel downregulation in the injured dorsal root ganglion after peripheral nerve injury. We demonstrated that blocking the peripheral nerve injury–induced increase in PRDM1 expression in the dorsal root ganglion restores the expression of the Kv4.3 channel,

reduces the hyperexcitability of injured dorsal root ganglion neurons, and attenuates nociception (fig. 10). As a limitation, our results were obtained in a mouse model rather than in patients with chronic pain; although experimentation in the mouse has the advantage of enabling detailed mechanistic insight, the applicability to human pain responses will require future verification. Furthermore, we have not elucidated mechanisms for PRDM1-dependent upregulation of several pain-associated genes that were identified in our analysis. The regulation of these genes may contribute to PRDM1 function in response to nociceptive pain hypersensitivity or other neural processes. Nevertheless, the new knowledge gained from this study advances our understanding of transcriptional mechanisms of peripheral nerve injury–induced nociception development and indicates that PRDM1 may represent a novel target for preventing and treating neuropathic pain.

Acknowledgments

The authors thank Professor Yuqiu Zhang, Ph.D. (Institutes of Brain Science, Fudan University, Shanghai, China), for her guidance with electrophysiologic and Ca^{2+} imaging experiments.

Research Support

This work was supported by the National Natural Science Foundation of China (grant Nos. 81500947 to C.W.; 31871076 and 31320103906 to T.B.; Beijing, China), Shanghai Municipal Science and Technology Major Project (No. 2018SHZDZX01; Shanghai, China), and ZJLab (China).

Competing Interests

The authors declare no competing interests.

Correspondence

Address correspondence to Dr. Behnisch: Mingdao Building, 138 Medical College Road, Shanghai, 200032, China. behnish@fudan.edu.cn. ANESTHESIOLOGY's articles are made freely accessible to all readers, for personal use only, 6 months from the cover date of the issue.

References

1. Devor M: Ectopic discharge in Abeta afferents as a source of neuropathic pain. Exp Brain Res 2009; 196:115–28
2. Laumet G, Garriga J, Chen SR, Zhang Y, Li DP, Smith TM, Dong Y, Jelinek J, Cesaroni M, Issa JP, Pan HL: G9a is essential for epigenetic silencing of K(+) channel genes in acute-to-chronic pain transition. Nat Neurosci 2015; 18:1746–55
3. Shinoda M, Fukuoka T, Takeda M, Iwata K, Noguchi K: Spinal glial cell line-derived neurotrophic factor infusion reverses reduction of Kv4.1-mediated A-type potassium currents of injured myelinated primary afferent neurons in a neuropathic pain model. Mol Pain 2019; 15:1744806919841196
4. Kim DS, Choi JO, Rim HD, Cho HJ: Downregulation of voltage-gated potassium channel alpha gene expression in dorsal root ganglia following chronic constriction injury of the rat sciatic nerve. Brain Res Mol Brain Res 2002; 105:146–52
5. Yu J, Angelin-Duclos C, Greenwood J, Liao J, Calame K: Transcriptional repression by blimp-1 (PRDI-BF1) involves recruitment of histone deacetylase. Mol Cell Biol 2000; 20:2592–603
6. Gyory I, Wu J, Fejér G, Seto E, Wright KL: PRDI-BF1 recruits the histone H3 methyltransferase G9a in transcriptional silencing. Nat Immunol 2004; 5:299–308
7. Küçük C, Iqbal J, Hu X, Gaulard P, De Leval L, Srivastava G, Au WY, McKeithan TW, Chan WC: PRDM1 is a tumor suppressor gene in natural killer cell malignancies. Proc Natl Acad Sci U S A 2011; 108:20119–24
8. Lin IY, Chiu FL, Yeang CH, Chen HF, Chuang CY, Yang SY, Hou PS, Sintupisut N, Ho HN, Kuo HC, Lin KI: Suppression of the SOX2 neural effector gene by PRDM1 promotes human germ cell fate in embryonic stem cells. Stem Cell Reports 2014; 2:189–204
9. Calame KL, Lin KI, Tunyaplin C: Regulatory mechanisms that determine the development and function of plasma cells. Annu Rev Immunol 2003; 21:205–30
10. Hernandez-Lagunas L, Choi IF, Kaji T, Simpson P, Hershey C, Zhou Y, Zon L, Mercola M, Artinger KB: Zebrafish narrowminded disrupts the transcription factor prdm1 and is required for neural crest and sensory neuron specification. Dev Biol 2005; 278:347–57
11. Gunasekaran M, Chatterjee PK, Shih A, Imperato GH, Addorisio M, Kumar G, Lee A, Graf JF, Meyer D, Marino M, Puleo C, Ashe J, Cox MA, Mak TW, Bouton C, Sherry B, Diamond B, Andersson U, Coleman TR, Metz CN, Tracey KJ, Chavan SS: Immunization elicits antigen-specific antibody sequestration in dorsal root ganglia sensory neurons. Front Immunol 2018; 9:638
12. Zimmermann M: Ethical guidelines for investigations of experimental pain in conscious animals. Pain 1983; 16:109–10
13. Bennett GJ, Xie YK: A peripheral mononeuropathy in rat that produces disorders of pain sensation like those seen in man. Pain 1988; 33:87–107
14. Han K, Zhang A, Mo Y, Mao T, Ji B, Li D, Zhuang X, Qian M, Chen S, Wang Z, Wang J: Islet-cell autoantigen 69 mediates the antihyperalgesic effects of electroacupuncture on inflammatory pain by regulating spinal glutamate receptor subunit 2 phosphorylation through protein interacting with C-kinase 1 in mice. Pain 2019; 160:712–23
15. Zhao ZQ, Chiechio S, Sun YG, Zhang KH, Zhao CS, Scott M, Johnson RL, Deneris ES, Renner KJ, Gereau

RW 4th, Chen ZF: Mice lacking central serotonergic neurons show enhanced inflammatory pain and an impaired analgesic response to antidepressant drugs. J Neurosci 2007; 27:6045–53
16. Bourquin AF, Süveges M, Pertin M, Gilliard N, Sardy S, Davison AC, Spahn DR, Decosterd I: Assessment and analysis of mechanical allodynia-like behavior induced by spared nerve injury (SNI) in the mouse. Pain 2006; 122:14.e1–14
17. Hargreaves K, Dubner R, Brown F, Flores C, Joris J: A new and sensitive method for measuring thermal nociception in cutaneous hyperalgesia. Pain 1988; 32:77–88
18. Brenner DS, Golden JP, Gereau RW 4th: A novel behavioral assay for measuring cold sensation in mice. PLoS One 2012; 7:e39765
19. Piao Y, Gwon DH, Kang DW, Hwang TW, Shin N, Kwon HH, Shin HJ, Yin Y, Kim JJ, Hong J, Kim HW, Kim Y, Kim SR, Oh SH, Kim DW: TLR4-mediated autophagic impairment contributes to neuropathic pain in chronic constriction injury mice. Mol Brain 2018; 11:11
20. Xu Y, Tian NX, Bai QY, Chen Q, Sun XH, Wang Y: Gait assessment of pain and analgesics: Comparison of the DigiGait™ and CatWalk™ gait imaging systems. Neurosci Bull 2019; 35:401–18
21. Li Z, Gu X, Sun L, Wu S, Liang L, Cao J, Lutz BM, Bekker A, Zhang W, Tao YX: Dorsal root ganglion myeloid zinc finger protein 1 contributes to neuropathic pain after peripheral nerve trauma. Pain 2015; 156:711–21
22. Lu Y, Jiang BC, Cao DL, Zhang ZJ, Zhang X, Ji RR, Gao YJ: TRAF6 upregulation in spinal astrocytes maintains neuropathic pain by integrating TNF-α and IL-1β signaling. Pain 2014; 155:2618–29
23. Robinson MD, McCarthy DJ, Smyth GK: edgeR: a Bioconductor package for differential expression analysis of digital gene expression data. Bioinformatics 2010; 26:139–40
24. Xu Y, Li P, Wang M, Zhang J, Wang W: Imaging the brain in 3D using a combination of CUBIC and immunofluorescence staining. Biomed Opt Express 2019; 10:2141–9
25. Choi S, Yu E, Hwang E, Llinás RR: Pathophysiological implication of CaV3.1 T-type Ca2+ channels in trigeminal neuropathic pain. Proc Natl Acad Sci U S A 2016; 113:2270–5
26. Liu ZY, Song ZW, Guo SW, He JS, Wang SY, Zhu JG, Yang HL, Liu JB: CXCL12/CXCR4 signaling contributes to neuropathic pain via central sensitization mechanisms in a rat spinal nerve ligation model. CNS Neurosci Ther 2019; 25:922–36
27. Xu W, Zhu M, Yuan S, Yu W: Spinal CXCL5 contributes to nerve injury-induced neuropathic pain via modulating GSK-3β phosphorylation and activity in rats. Neurosci Lett 2016; 634:52–9
28. Manjavachi MN, Passos GF, Trevisan G, Araújo SB, Pontes JP, Fernandes ES, Costa R, Calixto JB: Spinal blockage of CXCL1 and its receptor CXCR2 inhibits paclitaxel-induced peripheral neuropathy in mice. Neuropharmacology 2019; 151:136–43
29. Ergul S, Brunson CY, Hutchinson J, Tawfik A, Kutlar A, Webb RC, Ergul A: Vasoactive factors in sickle cell disease: *In vitro* evidence for endothelin-1-mediated vasoconstriction. Am J Hematol 2004; 76:245–51
30. Barr TP, Kam S, Khodorova A, Montmayeur JP, Strichartz GR: New perspectives on the endothelin axis in pain. Pharmacol Res 2011; 63:532–40
31. Pineda-Farias JB, Velázquez-Lagunas I, Barragán-Iglesias P, Cervantes-Durán C, Granados-Soto V: 5-HT2B receptor antagonists reduce nerve injury-induced tactile allodynia and expression of 5-HT2B receptors. Drug Dev Res 2015; 76:31–9
32. Chen Y, Shi Y, Wang G, Li Y, Cheng L, Wang Y: Memantine selectively prevented the induction of dynamic allodynia by blocking Kir2.1 channel and inhibiting the activation of microglia in spinal dorsal horn of mice in spared nerve injury model. Mol Pain 2019; 15:1744806919838947
33. Fan YX, Hu L, Zhu SH, Han Y, Liu WT, Yang YJ, Li QP: Paeoniflorin attenuates postoperative pain by suppressing matrix metalloproteinase-9/2 in mice. Eur J Pain 2018; 22:272–81
34. Miletic G, Hermes JL, Bosscher GL, Meier BM, Miletic V: Protein kinase C gamma-mediated phosphorylation of GluA1 in the postsynaptic density of spinal dorsal horn neurons accompanies neuropathic pain, and dephosphorylation by calcineurin is associated with prolonged analgesia. Pain 2015; 156:2514–20
35. Zhang Y, Gong K, Zhou W, Shao G, Li S, Lin Q, Li J: Involvement of subtypes γ and ε of protein kinase C in colon pain induced by formalin injection. Neurosignals 2011; 19:142–50
36. Chien LY, Cheng JK, Chu D, Cheng CF, Tsaur ML: Reduced expression of A-type potassium channels in primary sensory neurons induces mechanical hypersensitivity. J Neurosci 2007; 27:9855–65
37. Viatchenko-Karpinski V, Ling J, Gu JG: Down-regulation of Kv4.3 channels and a-type K+ currents in V2 trigeminal ganglion neurons of rats following oxaliplatin treatment. Mol Pain 2018; 14:1744806917750995
38. Zemel BM, Ritter DM, Covarrubias M, Muqeem T: A-type KV channels in dorsal root ganglion neurons: Diversity, function, and dysfunction. Front Mol Neurosci 2018; 11:253
39. Pasqualucci L, Compagno M, Houldsworth J, Monti S, Grunn A, Nandula SV, Aster JC, Murty VV, Shipp MA, Dalla-Favera R: Inactivation of the PRDM1/BLIMP1 gene in diffuse large B cell lymphoma. J Exp Med 2006; 203:311–7

40. Chen YC, Auer-Grumbach M, Matsukawa S, Zitzelsberger M, Themistocleous AC, Strom TM, Samara C, Moore AW, Cho LT, Young GT, Weiss C, Schabhüttl M, Stucka R, Schmid AB, Parman Y, Graul-Neumann L, Heinritz W, Passarge E, Watson RM, Hertz JM, Moog U, Baumgartner M, Valente EM, Pereira D, Restrepo CM, Katona I, Dusl M, Stendel C, Wieland T, Stafford F, Reimann F, von Au K, Finke C, Willems PJ, Nahorski MS, Shaikh SS, Carvalho OP, Nicholas AK, Karbani G, McAleer MA, Cilio MR, McHugh JC, Murphy SM, Irvine AD, Jensen UB, Windhager R, Weis J, Bergmann C, Rautenstrauss B, Baets J, De Jonghe P, Reilly MM, Kropatsch R, Kurth I, Chrast R, Michiue T, Bennett DL, Woods CG, Senderek J: Corrigendum: Transcriptional regulator PRDM12 is essential for human pain perception. Nat Genet 2015; 47:962
41. Wang C, Song S, Zhang Y, Ge Y, Fang X, Huang T, Du J, Gao J: Inhibition of the Rho/Rho kinase pathway prevents lipopolysaccharide-induced hyperalgesia and the release of TNF-α and IL-1β in the mouse spinal cord. Sci Rep 2015; 5:14553
42. Wang C, Wang H, Pang J, Li L, Zhang S, Song G, Li N, Cao J, Zhang L: Glial cell-derived neurotrophic factor attenuates neuropathic pain in a mouse model of chronic constriction injury: Possible involvement of E-cadherin/p120ctn signaling. J Mol Neurosci 2014; 54:156–63
43. Aldrich R: Ionic channels of excitable-membranes. Science 1985; 228:867–8
44. Duan KZ, Xu Q, Zhang XM, Zhao ZQ, Mei YA, Zhang YQ: Targeting A-type K(+) channels in primary sensory neurons for bone cancer pain in a rat model. Pain 2012; 153:562–74
45. Usoskin D, Furlan A, Islam S, Abdo H, Lönnerberg P, Lou D, Hjerling-Leffler J, Haeggström J, Kharchenko O, Kharchenko PV, Linnarsson S, Ernfors P: Unbiased classification of sensory neuron types by large-scale single-cell RNA sequencing. Nat Neurosci 2015; 18:145–53

ANESTHESIOLOGY REFLECTIONS FROM THE WOOD LIBRARY-MUSEUM

Shaker Anodyne: Teetotalers' Valerian Elixir

A religious group founded in England in the 1740s, the Shakers were organized in the United States by the 1780s and lived in communes from upstate New York and New England to urban Philadelphia and the Midwest. A uniquely celibate sect of Christian teetotalers, their ecstatic singing and dancing at worship had earned them the sobriquet of "Shaking Quakers," or Shakers. Up through the 1890s, their North Enfield (*bottom*, "Nth Enfield / N.H.") community in New Hampshire compounded "Brown's Pure Extract of English Valerian," better known as "Shaker Anodyne" (*top*). The root of the English, not American, Valerian plant contained a soporific and analgesic volatile oil. Likely contributing to Shaker Anodyne's popularity was the fact that the root was mixed into a strongly alcoholic elixir spiked with opium and an herb widely regarded as Satanic, containing hyoscine and atropine: henbane. (Copyright © the American Society of Anesthesiologists' Wood Library-Museum of Anesthesiology.)

Melissa L. Coleman, M.D., Penn State College of Medicine, Hershey, Pennsylvania, and Jane S. Moon, M.D., University of California, Los Angeles, California.